C. Files

Report No. IE-116

Metallurgical Examination and Stress Evaluation of Recirculation Inlet Nozzle Safe-End Cracking at Duane Arnold Energy Center Iowa Electric Light & Power Co.

Dr. S. Weiss

R. S. Dean

PARAMETER, Inc.

V. Pasupathi

G. P. Smith

D. R. Farmelo

J. S. Perrin

Battelle Columbus Laboratories

Prepared for

U. S. Nuclear Regulatory Commission

NOTICE

Available from
U. S. Nuclear Regulatory Commission
Washington, D. C. 20555

IE-116

Distribution	Copies
Nuclear Regulatory Commission Technical Assistance Branch Office of Inspection and Enforcement	40
PARAMETER, Inc.	
File Copy	1
S. Weiss	1

Report of

Metallurgical Examination and Stress Evaluation of Recirculation Inlet Nozzle Safe-End Cracking

at

Duane Arnold Energy Center

Iowa Electric Power Company

Report No. IE-116, March 16, 1979

Prepared for: United States Nuclear Regulatory Commission
Office of Inspection & Enforcement

NRC Contract 05-77-186
PAR: NRC-IE-78/79, Task 03

WISCONSIN
ROBERT S.
DEAN
E-8826
ELM GROVE,
WIS.
PROFESSIONAL ENGINEER

By: Robert S. Dean
Robert S. Dean, P.E.

Stanley Weiss
Dr. S. Weiss, P.E., Consultant

Walter J. Foley
Walter J. Foley, P.E.

PARAMETER, Inc.
Consulting Engineers
Elm Grove, Wisconsin

SECTION I

Abstract

Presented is a report of a metallurgical investigation and stress analysis study of a cracked safe end from a recirculation inlet nozzle from the reactor at Duane Arnold Energy Center. The work was coordinated by PARAMETER, Inc. at the request of the Nuclear Regulatory Commission. The metallurgical investigation was performed by Battelle Columbus Laboratories, and the stress analysis study was made by PARAMETER staff members. Results correlate well with a parallel investigation of a companion nozzle safe end directed by the Iowa Electric Light and Power Company at Southwest Research Institute. The cracking is identified as intergranular stress corrosion cracking. The crack originated in the weld heat-affected zone at the tight crevice formed by the safe end and thermal sleeve joint, and progressed radially outward from 30 to 80 percent through the Inconel safe end wall. The crevice provided a location in which contaminant build up was able to occur, as well as a region in which high localized stresses were concentrated. Review of the replacement safe end design shows elimination of the tight crevice and reduction of stresses to levels thought to be low enough to avoid recurrence of the cracking.

CONTENTS

SECTION II

Introduction

Task Order #3 on Parameter NRC Contract #05-77-186, issued by The Office of Inspection and Enforcement of NRC, requested assistance and consultation services for a metallurgical evaluation of a nozzle safe end from the reactor vessel at Duane Arnold Energy Center. This safe end was from a companion nozzle to one that had cracked-through, and was being investigated under the jurisdiction of the Licensee, Iowa Electric Light and Power Company. The main intent of the parallel Parameter study was to verify findings of the Licensee investigation.

In addition, the task order requested assistance in review and evaluation of the Licensee's failure analysis of the cracked-through safe end, and assistance in review of the Licensee's design basis analysis of the recirculation inlet nozzle.

The Duane Arnold Energy Center is a nuclear power generation plant with a boiling water reactor, operated by Iowa Electric Light and Power Company, and located at Palo, Iowa, near the City of Cedar Rapids. General Electric was the reactor designer, and Chicago Bridge & Iron, CBI Nuclear, was the fabricator. The reactor was assembled on site by CBI.

The subject safe ends are from the recirculation inlet nozzles of the reactor, of which there are eight, all of which had indications of cracking as found by non-destructive inspection at the site after leakage had been detected from the cracked-through safe end. The nozzle designation for the Parameter investigation is N2E.

The N2E safe end as cut from the vessel was shipped without decontamination to Battelle Columbus Laboratories for the metallurgical studies. This was done with coordination at the site by Mr. Raymond Sutphin, Quality Assurance Engineer, of Parameter.

Radiographs of the nozzle N2E safe end, taken on site prior to cutting out the section, were carried to Parameter by Mr. Sutphin. These radiographs were reviewed at Parameter by Mr. Kenneth Ristau, Consultant for non-destructive testing, and Dr. S. Weiss, Consultant for metallurgy, and during this review, locations were selected for sectioning for metallurgical study.

The metallurgical investigation at Battelle was conducted under the direction of Parameter Consultant, Dr. Stanley Weiss. The Battelle report is Exhibit A of this report. Dr. Weiss' evaluation, conclusions, and comments are Section IV of this report.

The review of the original and replacement design analyses of the recirculation inlet nozzle were made by Parameter staff engineers. The discussion is included herein as Section VI and VII. Stress tabulations, calculations, and comparisons are included as Attachment #1.

A summary of the more significant findings and conclusions are given following this introduction.

SECTION III

Summary of Findings

1. Metallurgical Analysis

   1.1 The mechanism and mode of cracking is identified as intergranular stress corrosion cracking.

   1.2 The crack originated at the crevice formed by the safe end and thermal sleeve, and extended a full 360° circumferentially around the safe end.

   1.3 Sulfur was observed on the fracture surfaces and adjoining crevices.

   1.4 The crack originated in and propagated from 30 to 80 percent through the safe end wall from the weld heat-affected zone of the safe end/thermal sleeve weld joint.

   1.5 The heat-affected zone exhibits partial re-solutionizing of the grain boundaries, which exhibit significant sensitization in the Inconel base material.

   1.6 No corrosion pitting attack or multiple cracking was observed. Only a single crack was found.

2. Review of Stress Analysis, Original Design

   2.1 The original stress analysis identified the safe end/thermal sleeve joint as a high stress location, due to the stress concentration effect of the crevice.

   2.2 Fatigue analysis at this location per Code with added conservatism showed that the design was acceptable to the Code.

   2.3 Normal operating loading conditions cycle stresses to over yield strength of the material at the crack location, due to the stress concentration effect.

   2.4 The original design was acceptable from a stress and fatigue analysis standpoint for the extreme sudden recirculation pump startup. This transient was never experienced in actual plant operation.

3. Review of Stress Analysis, Replacement Design

   3.1 Safe end operational loading stress levels are reduced to approximately 50% of those of the original design.

   3.2 Residual stress from the safe end/thermal sleeve weld is reduced to below yield stress level.

   3.3 Normal operation loading stress, including stress concentration, cycles within the yield strength range of the material.

   3.4 Extreme transient stress range, including stress concentration, only slightly exceeds yield strength range. Fatigue evaluation shows this to be well within Code acceptable limits.

SECTION III - Continued

Conclusions

1. The metallurgical investigation of the N2E safe end at Battelle Columbus Laboratories under Parameter direction are in close agreement with the findings of the Licensee directed investigation of the cracked-through N2A safe end conducted at Southwest Research Institute.

2. Main factors contributing to the intergranular stress corrosion cracking of the original safe end design appear to be:

   2.1 Presence of the tight crevice, causing:

      2.1.1 Stress concentration

      2.1.2 Contaminant build-up

   2.2 Relatively high stresses at cracking location, although not over code allowable.

   2.3 Susceptibility of the Inconel to cracking due to the sensitization by heat treatment and welding.

3. The proximity of the repair welding on the O.D. of the original safe end appears to have had no effect on the cracking.

4. The importance of residual stress from welding is an unresolved question. It is a possibility that residual stress could have been a major source of stress to <u>initiate</u> the cracking, but the stress analysis review shows that pressure and thermal load stresses were high enough for intergranular stress corrosion cracking to occur without residual stress being present initially.

5. The replacement design accomplishes objectives in:

   5.1 Reduction of stresses from operating loads.

   5.2 Reduction of residual stresses from the safe end/thermal sleeve weld.

   5.3 Elimination, or at least drastic reduction, of the objectionable effects of a tight crevice by replacement of the crevice with an annulus with controlled dimensions.

SECTION IV

Review and Conclusions

from

Battelle Metallurgical Report

by

Dr. S. Weiss, P.E.
Metallurgical Consultant

to

PARAMETER, Inc.

Review and Conclusions from Battelle Metallurgical Report

by Dr. S. Weiss

In accordance with the request of the Nuclear Regulatory Commission, a metallurgical examination has been performed on safe end N2E at the Battelle Laboratory under the direction of PARAMETER, Inc. The objectives of this study were to:

a. Conduct an independent study to compare with a parallel study performed by the Licensee on a companion safe end section containing a through wall crack.

b. Determine the mechanism and mode of failure in safe end N2E.

c. Provide assistance in the review and evaluation of the Licensee's failure analysis of a through-wall cracked safe end removed from a companion BWR Nozzle.

and d. Provide assistance in the review of the Licensee's design analysis of the recirculation inlet nozzle.

The work at Battelle is now completed and has been reported on in the final January 1979 Battelle Data Report entitled "Examination of Inconel Safe End From Duane Arnold" by V. Pasupathi, et al.(Exhibit A)

Additionally, considerable information and numerous inputs into the understanding of the problem were gained by interim visits to Battelle Laboratory during the course of the investigation, visiting the South-West Research Institute (SwRI) to review their preliminary findings on behalf of the Licensee and attending numerous meetings between the Licensee, General Electric, NRC, Battelle, SwRI and PARAMETER, Inc.

The most relevant findings from the Battelle study are:

1. The mechanism and mode of cracking in Nozzle N2E is identified as intergranular stress corrosion cracking.

2. The cracks observed originate and propagate from a relatively tight crevice which ranges in length from 0.2 to 0.3 in. and ranges in gap size from 0.002 to 0.005 in.

3. Sulfur was observed on the fracture surfaces and adjoining crevices. Concentration profiles show that the intensity of sulfur was found to increase towards the crack tip. The level of intensity of sulfur observed in these studies revealed that the sulfur found was present as a contaminant and not as an inherent constituent of the base materials.

4. The cracks originate in and propagate from the weld heat-affected zone of the weld joining the Inconel 600 thermal sleeve to the Inconel 600 safe end. The heat-affected zones of these welds exhibit only partial re-solutionizing of the grain boundaries, which exhibited significant sensitization in the initial safe end base material prior to welding.

5. No corrosion pitting attack or multiple cracking was observed in any of the specimens analyzed. In each specimen only a single crack was found to originate in the heat-affected zone.

6. No apparent evidence of fatigue or cyclic loading was observed. However, this does not preclude the possibility of crack propagation by low cycle corrosion fatigue in addition to that attributable to IGSCC, since these two modes of fracture may have similar fractographic appearances in this application.

From these findings it is concluded that the major factors contributing to cracking and failure of these nozzles appears to be:

A. The presence of a tight crevice within which localized chemical reactions and conditions are occurring.

B. The presence of high localized applied stresses of yield strength magnitude at the safe end weld.

C. The presence of high localized residual welding stresses at the same location resulting from field welding of the thermal sleeve to the safe end.

D. The presence of an adverse sulfur rich chemical environment which is known to promote stress corrosion cracking in high nickel base alloys. Examination of the performance history of the Duane Arnold Reactor may indicate the potential source of this contaminant.

These findings appear to agree with the preliminary report of studies performed at SwRI on behalf of the Licensee. The final report from SwRI was not reviewed and thus a direct comparison with the Battelle final report has not been made. However, it is believed that the findings of each of the studies essentially corroborate one another.

The stress relieved repair welds introduced to the safe ends prior to final field fabrication did not appear to be a contributing factor to the cracking problem experienced. The thermal sleeve and safe end were both sensitized exhibiting discrete precipitated carbides at the grain boundaries. Although these base materials exhibited sensitized conditions, no stress corrosion cracking or corrosion pitting was observed in either material at the faying interfaces within the crevices adjacent to the weld heat-affected zones which contained the crack.

The findings of the study confirmed that re-design concepts must take the following recommendations into consideration:

- Minimize applied and residual welding stresses to a safe level by revising the structural design.

- Eliminate crevices and crevice conditions in welded joints.

Study of the cracking problem experienced in the Inconel 600 safe ends at Duane Arnold has raised numerous important questions which can be answered only by formalized research and developmental programs. Among those factors and questions which appear to be of vital importance are:

- The role of both the applied stresses and residual welding stresses in causing these failures.

- What geometry constitutes a crevice?

- What is the influence of specific BWR environments that can potentially cause IGSCC in the presence of a crevice, weld, and stress condition?

- Which non-destructive test methods are most reliable for detecting initiation and propagation of cracks such as were observed in these studies?

SECTION V

Comments on Metallurgical Findings at Battelle and Southwest Research

by

R. S. Dean, P.E.
Staff Engineer
PARAMETER, Inc.

Comments on Metallurgical Findings

by R. S. Dean, P.E.
PARAMETER Staff Engineer

Cause of Failure

Ample evidence was found that intergranular stress corrosion cracking (IGSCC) of the inconel safe end material was responsible for the cracks in the Duane Arnold recirculation inlet piping. This is well presented and stated in the Southwest Research Institute interim report (Ref.1,pg. 40) and is substantiated by the Battelle Columbus Laboratory report (Ref.2,pg.43).

Conditions Required for IGSCC

Reference (1) infers (pg.40) and Reference (3)(pg.2-1) states that three conditions are required to initiate IGSCC: 1) a susceptible material, 2) an aggressive environment, and 3) stress. It seems agreed that yield stress level is required locally to the zone of crack initiation (Ref.1, pg.40; Ref.3,pg.5-1).

Conditions Causing IGSCC at Duane Arnold:
Material Susceptibility

Reference (1) sites published data supporting susceptibility of Inconel 600 to IGSCC in high purity water environments (Ref.1,pg.40).

Analyses of the chemical composition of the safe end material verify that it is Inconel 600 (Ref.1,pg.40; Ref.2,pg.43). Cracking occurred in both sensitized and re-solution treated zones in the SwRI study (Ref. 1,pg.40), and only in the partially re-solution treated zone in the Battelle findings (Ref.2,pg.43).

Crevice and Aggressive Environment

The presence of the crevice is agreed by References (1) and (2) to be a major contributing factor to the cracking. All cracking initiated near the tip of the crevice formed by the safe end/thermal sleeve joint, with only one initiation location at any given radial section. No incipient intergranular attack, pitting, or other evidence of significant chemical attack was found present along the surface of the crevice by either investigation (Ref.1,pg.39, Ref.2,pg.43).

Reference (1) sites the crevice as an entrapment location for concentrations of the necessary corrosive environment for IGSCC (Ref.1,pg.40).

Stress

Both the SwRI and Battelle reports describe the safe end cracking as relatively regular in depth circumferentially a full 360°, and that crack progression through the base material shows no evidence of being step-wise in nature (Ref.1,pg.40; Ref.2,pg.43). Initial cracking progressed along a single line for some small percentage of depth, and then some intergranular branching occurred in the deeper sections, possibly

Comments on Metallurgical Findings - continued

Stress - continued

indicating relief of the initial very large tensile stresses by the first straight length of crack. Reference (1) expresses the opinion that this initial stressed condition is due primarily to the residual stresses caused by the un-stress-relieved welding of the thermal sleeve to the safe end (Ref.1,pg.42). After this stress was relieved by the initial crack, normal load stresses caused by pressure, temperature, and other mechanical loads present, would contribute stresses high enough at the tip of the crack to continue the progression. Even though primary and secondary load stresses could be relatively low, peak stress, due to the stress concentration by the presence of the crack, could be expected to exceed elastic limits and continue to propagate the crack.

SECTION VI

Review of Stress Levels, Original Design

and

SECTION VII

Review of Stress Levels, Replacement Design

by

R. S. Dean, P.E.
Staff Engineer
PARAMETER, Inc.

SECTION VI

Review of Stress Levels, Original Design

by R. S. Dean, P.E.

(A sketch of the safe end/nozzle geometry is shown on Page 3 of Attachment 1.)

An adequate stress analysis per code was made at the time of design by Chicago Bridge & Iron in Reference (4). In this analysis, the section through the safe end at the tip of the crevice was identified as the highest stressed section of the nozzle assembly. A fatigue analysis was made at point 13 (Ref.4,F8-14 thru 30) on the safe end at the tip of the crevice. A theoretical stress concentration factor of 4 was used for the analysis at this point, and a usage factor of .515 was calculated.

In the code (Ref.5,pph.N-415.3,pg.28 and Ref.6,pph.NB-3222.4-e(2),pg.64) evaluation of stresses at structural discontinuities, the statement is made, "Except for the case of crack-like defects, no fatigue strength reduction factor greater than five need be used." On the basis that the crevice is quite crack-like, it is felt that a factor of at least five should have been used, since no experimental or other basis for using four is given.

In order to make a comparison using factors of both 4 and 5, Attachment 1 presents a fatigue analysis made strictly per the ASME Code procedure (Ref.5,pph.N-415.2). The original analysis used an elastic-plastic method per Reference (7) which modifies the alternating stress for use with Code design fatigue curves (figs.N-415(a),(b)), and arrives at more conservative results.

Also, it appears that the design fatigue curve N-415(b) as in the 1968 edition of the Code (Ref.5) was used in the original analysis. This curve was corrected in the summer 1968 Code addenda to agree with the curve in the 1965 edition of the Code, which also agrees with the current (1977) edition. However, the corrected curve is less conservative than the one used (1968). Attachment 1 uses the corrected curve.

The results of the fatigue analysis of Attachment 1 show that the cumulative usage factor is quite low; 0.09 for k = 4, 0.190 for k = 5. Both results are less than the .515 with k = 4 calculated in the original report, and much less than the Code allowable of 1.0. This clearly makes the original design acceptable on the basis of fatigue analysis per Code.

Also presented in Attachment 1 are comparisons to yield strength of point 13 axial stress and stress intensity range of the three cyclic conditions used for fatigue analysis. According to the operation history of Duane Arnold (Ref.9, Attachment B), the sudden recirculation pump startup (Transient 1) was never experienced, so the very high stresses (strains) of this transient never occurred. Axial stress from hydrotest is less than yield strength, and stress intensity range from hydrotest is well within the 3 Sm Code allowable. However, add to this the residual stress expected as a result of the sleeve-to-safe end weld, which is of the order of yield stress (see Att.1,pg.14), and the stress at point 13 is cycled through a shakedown at first pressurization. This might initiate cracking, but normally it would not be expected to do so because of the ductile nature of the Inconel.

Review of Stress Levels, Original Design - Continued

A plot of cycling axial stress (without peak stress) at point 13 is shown on Page 14 of Attachment 1, assuming an initial cyclic history of the nozzle very roughly based on reported history (Ref.9, Att.B). The plot indicates that after an initial shakedown of stress from residual through two hydrotests and shutdowns, cycling axial stress (without peak stress) of the milder transients and normal startups and shutdowns would fluctuate thereafter with tensile yield stress as a maximum. One cycle of the extreme cold pump startup is shown to show the shift in mean stress that it would cause for subsequent milder cycling. This transient did not occur in the actual history, as mentioned earlier, but is of interest for comparison with the analysis of the replacement design.

The presence of the crevice, however, creates stress concentration peak stresses as tabulated for the various conditions on page 10 of Attachment 1 (also Ref.4,pg.F8-26). The tabulation shows that even normal startup and shutdown transients cause point 13 psuedo-elastic stress to exceed yield strength, and cause local plastic strains to occur. The more severe cool-down-warmup transient #2 causes greater strains, of course. These strains are local on the safe end I.D., and do not cause distortion of the full cross-section.

Stress cycling as described in the previous paragraph is normal Code design practice for high peak stress locations in ductile materials, keeping the cumulative usage factor less than 1.0. However, this local strain cycling, along with steady state (sustained) stress condition at yield stress level, in the presence of susceptible material and corrosive environment, provides the conditions which promote stress corrosion cracking.

It could be concluded from the plots of cyclic stress that the presence of the initial residual stress from welding is immaterial. The stress mechanism for stress corrosion cracking is present whether or not there is initial residual stress. Normally, with a ductile material, it is unlikely that the residual stress would be severe enough to initiate the cracking immediately. Also, the corrosive conditions required for intergranular stress corrosion cracking would not have been present initially when the weld was made, so it is doubtful that the residual stress from welding initiated the crack.

The relative uniformity of the crack around the entire periphery of the safe end, as found by Refs. 1 & 2, leads these references to the conclusion that the residual stress from welding was the principal contributor to cracking, because of the relatively axisymmetric nature of residual stress from the sleeve to safe end weld. The main load stresses are from pressure and temperature, and also are axisymmetric in nature. The non-axisymmetric stresses from piping loads produce stress of some lesser magnitude, and, in addition, although it is not analyzed specifically, the direction of the piping loads would be expected to vary during temperature and pressure cycling, causing principal stress directions to vary. There would be a resulting <u>tendency</u> for this also to contribute to the cracking all around the periphery, rather than in one circumferential location only, as might be thought would result from just piping load stresses.

SECTION VII

Review of Stress Levels, Replacement Design

by R. S. Dean, P.E.

On page 11 of Attachment 1, comparisons are made between stresses at the point on the inside wall of the safe end (point 130) and corresponding point 13 of the original design. The replacement design avoids the sharp crevice by substituting an annulus with controlled radii at the tip, keeping the stress concentration much lower, and the safe end wall is thicker at this section (.96 in. vs. .57 inches on the original). These changes are responsible for reducing the stress levels by nearly 50 percent. Fatigue analysis results in a very low cumulative usage factor of .002, compared to .09 for the original design, and to maximum Code allowable of 1.0.
The replacement design also reduces the level of residual stress in the safe end wall by removing the weld from direct attachment to the wall, as with the original design. The flexibility of the joint to the thermal sleeve allows elastic displacement to accommodate radial weld shrinkage, and residual stress is kept below yield stress (pg.11 of Att.1).

For a comparison with cyclic axial stresses of the original design, use is made of the superpositioned total of axial stress from the various loadings calculated in Ref. 8 for the replacement design (see Att. 1, pg. 12). These are taken at a critical time during the extreme sudden pump startup transient. Primary plus secondary axial stress is plotted, page 15, using stress without thermal component for normal startup and shutdown cycles. The plot shows stress shakes down to the range between yield stress limits, whereas, for the original design, the last cycle plotted on page 14 shows the primary plus secondary stress (psuedo-elastic) far exceeds the yield stress.

Total stress, including peak stress, using the extreme pump startup transient, only slightly exceeds yield stress (Att.1,pg.13). For the normal controlled startup and shutdown cycles, total stress remains within the yield stress range, which it did not do in the original design. It is reasonably certain that total stress for the mild heatup and cooldown transients also would cycle within the elastic range.

SECTION VIII

References

1. Burghard, H.C., Jr., Metallurgical Investigation of Cracking in a Reactor Vessel Nozzle Safe-End, Interim Report, SwRI Project 02-5389-001, Southwest Research Institute, October 20, 1978.

2. Pasupathi, V., Smith, G.P., Farmelo, D.R., and Perrin, J.S., Examination of Inconel Safe End from Duane Arnold, Battelle Columbus Laboratories, Final Report, Project BCL-585-9, January, 1979.

3. Lemaire, J.C., Ranganeth, S., Prevention of Stress Corrosion by Limitation of Applied Static Loads in BWR Piping and Components, General Electric, DRF6880052, Nuclear Energy Engineering Division, San Jose, California, September, 1978.

4. Stress Analysis Report of Original Recirculation Inlet Nozzle N2 (including Safe-end Stresses), Sections T8 (Thermal Analysis, S8 (Stress Analysis), F8 (Fatigue Analysis), Chicago Bridge & Iron, Rev. 1, November, 1971.

5. ASME Boiler and Pressure Vessel Code, Section III, Nuclear Vessels, 1968, with Summer 1968 Addenda.

6. ASME Boiler and Pressure Vessel Code, Section III, Division 1, Nuclear Power Plant Components, Sub-section NB, Class 1 Components, 1977.

7. Tagart, S. W., Plastic Fatigue Analysis of Pressure Components, ASME Paper No. 68-PVP-3, American Society of Mechanical Engineers.

8. Stress Report, Recirc Inlet Nozzle Safe End Replacement, Duane Arnold Nuclear Plant, CBI Nuclear Company, August 10, 1978.

9. Responses to five questions concerning The Duane Arnold Energy Center Recirculation Inlet Nozzle Analysis, letter to J. G. Keppler, U.S. NRC, Region III, from Lee Liu, Sr. V.P., Engineering, Iowa Electric Light and Power Company, July 26, 1978, IE-78-1137.

10. Recirculation Inlet Safe End Repair Program, Duane Arnold Energy Center, Iowa Electric Light and Power Company, IE-78-1782, December 8, 1978.

11. Drawing, Original Design, Thermal Sleeves for Recirculation Inlet Nozzles Mark N2 A/H, Chicago Bridge and Iron Company, Contract 68-2967, Drawing No. 32, Sheet 7, Purchaser's No. 205H1289.

12. Drawings, Replacement Design:
    1. Reactor Vessel, General Electric Drawing No. 794E904, Sheet 2, Revision 0.
    2. Safe End, General Electric Drawing No. 112D2504, Rev. 0.
    3. Adapter, Thermal Sleeve, General Electric Drawing No. 137C7284, Rev. 0.

SECTION IX

Exhibits and Attachments

Exhibit A:

Battelle Columbus Laboratories
Report BCL-585-9
January 1979

Examination of Inconel Safe End from Duane Arnold

by: V. Pasupathi
G. P. Smith
D. R. Farmelo
J. S. Perrin

Attachment No. 1:

Stress Tabulations, Calculations, and Comparisons for Safe End/Thermal Sleeve Joint Location in Reactor Nozzle N2 at Duane Arnold Energy Center

by: R. S. Dean and W. J. Foley
PARAMETER, Inc.

Attachment No. 1
to Report IE-116

Stress Tabulations, Calculations and Comparisons for Safe End/Thermal Sleeve Joint Location in Reactor Nozzle N2 at Duane Arnold Energy Center

Iowa Electric Light and Power Company

Prepared for: U. S. Nuclear Regulatory Commission
Office of Inspection & Enforcement

NRC Contract 05-77-186
PAR: NRC-IE-78/79, Task 03

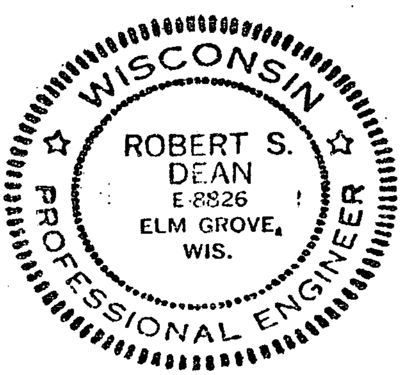

by: PARAMETER, Inc.
Consulting Engineers
Elm Grove, Wisconsin

Robert S. Dean, P.E.

Checked by: Walter J. Foley, P.E.

Introduction

Sketches of original and replacement safe end design are shown on page 3.

For the original design, a re-calculation of fatigue analysis at point 13 is presented, following 1968 code procedure, and using the code fatigue curve of the summer 1968 addenda. Strength reduction factors of both 4 and 5 are used for comparison of resultant usage factors.

Longitudinal stresses are compared with yield strength for each significant cyclic load condition. Cycling stress intensity range is compared to 3 Sm limit and is roughly plotted to illustrate shakedown and the effect of adding in residual stress estimate.

Stresses from the replacement design report for the comparable location on the new safe end are tabulated and plotted for comparison to the original design.

Summary and Discussion

See Sections III, VI, and VII of report IE-116.

References

See Section VIII of report IE-116.

Comments on Safe End Replacement Design

A comparison of the sketches of the two designs for the safe end show that the replacement design accomplishes the following:

1. The wall thickness is increased in the tapered section at the thermal sleeve attachment location which reduces stresses from operating loads.

2. The sleeve-to-safe-end weld joint is separated from the pressure boundary wall of the safe end, preventing any possible cracking in the weld heat affected zone from propagating through the pressure boundary wall. Weld location on the relatively flexible projection from the safe end accommodates circumferential weld shrinkage, reducing residual stresses from welding.

3. The crack-like crevice is eliminated, and is replaced with an annulus of controlled dimensions. This reduces the stress concentration by over 50%, and substantially reduces the tendency to trap corrosive contaminants at this location.

BY R.S.D. DATE 3/15/79
CHK'D BY WJF DATE 4-16-79
PARAMETER NRC-03

ORIGINAL DESIGN
(REF. 11)

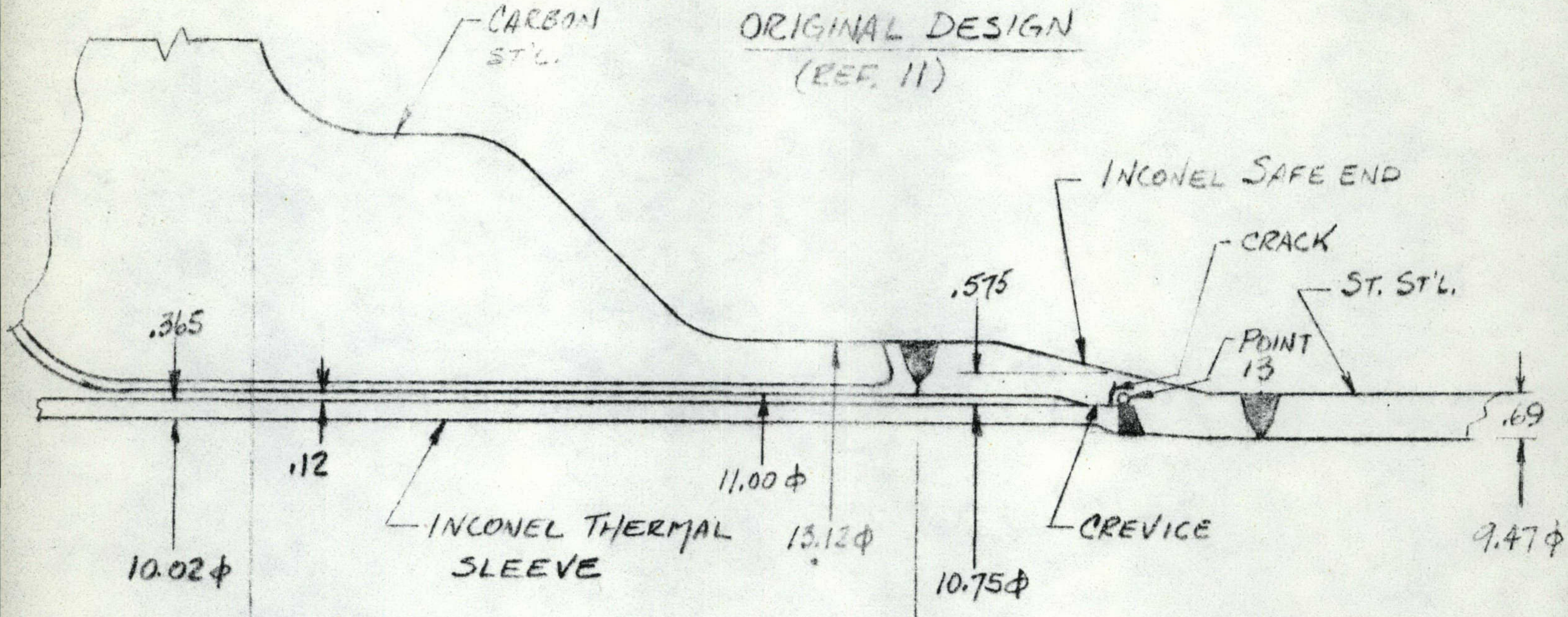

REPLACEMENT DESIGN
(REF. 12)

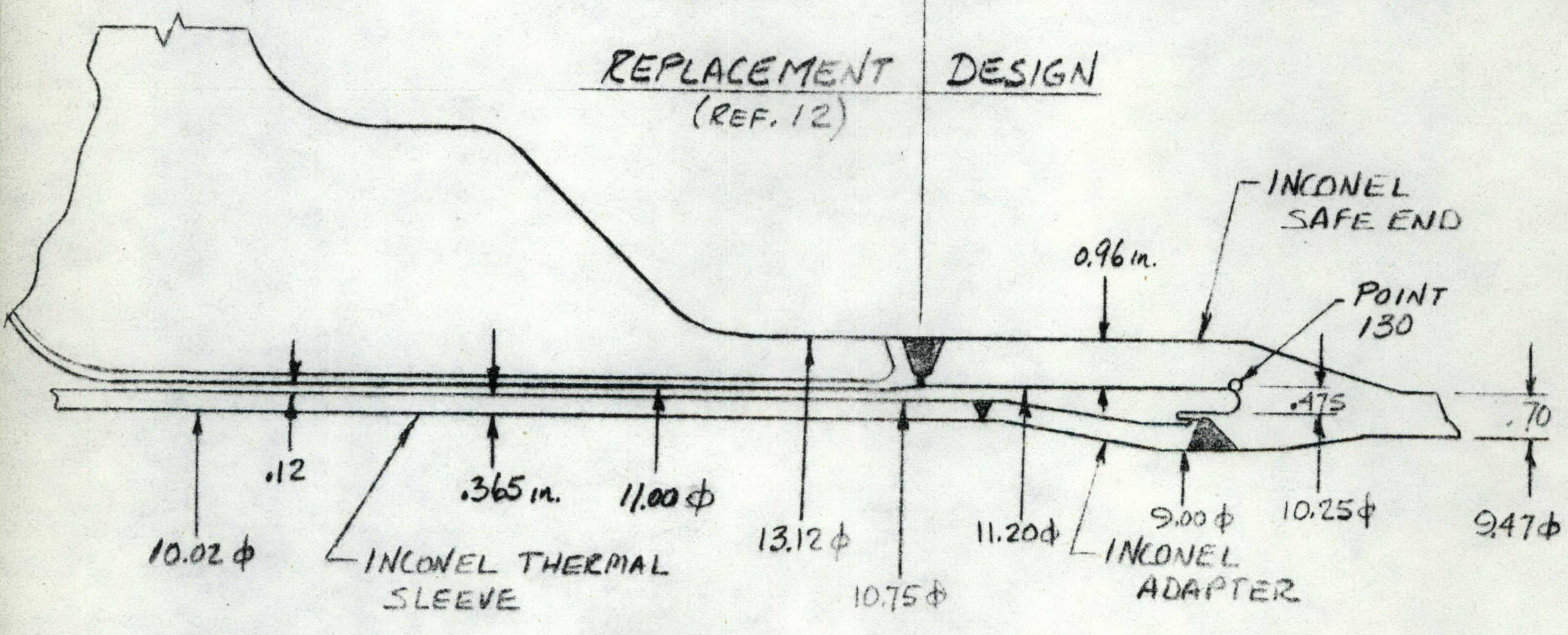

N-2 SAFE END ORIGINAL AND REPLACEMENT DESIGNS — DUANE ARNOLD ENERGY CENTER

SCALE ~ APPROX. 1/4

REVIEW OF CALCULATED STRESSES AT TIP OF CREVICE AT SAFE-END/THERMAL SHIELD WELD JOINT.

THE CRACKING OCCURED IN THE SAFE-END MATERIAL, INCONEL 600, SB-166 (EQUIV.), LISTED BY THE CODE (REFS. 5 & 6) AS HAVING FOLLOWING PROPERTIES AT 575°F:

MIN. YIELD STRENGTH: S_y = 28100 PSI.

DESIGN STRESS INTENSITY: S_m = 23300 PSI.

ELASTIC MODULUS: $E = 29.3 \times 10^6$ PSI.

STRESS VALUES ARE TAKEN FROM REF. 4 AT ANALYSIS LOCATION, POINT 13 (REF. 4, PP. F8-19 THRU 26).

STRESS NOMENCLATURE: (+) TENSION, (−) COMPRESSION

σ_ϕ = LONGITUDINAL (AXIAL) STRESS

σ_θ = HOOP (CIRCUMFERENTIAL) STRESS

σ_r = RADIAL STRESS

S = STRESS INTENSITY

S_r = " " RANGE

S_a = ALTERNATING STRESS INTENSITY

A RE-CALCULATION OF FATIGUE ANALYSIS AT POINT 13 IS PRESENTED, FOLLOWING 1968 CODE PROCEDURE, AND USING THE CODE FATIGUE CURVE OF THE SUMMER 1968 ADDENDA. STRENGTH REDUCTION FACTORS OF BOTH 4 AND 5 ARE USED FOR COMPARISON OF RESULTANT USAGE FACTORS. (pp. 5-7)

LONGITUDINAL STRESSES ARE COMPARED WITH YIELD STRENGTH FOR EACH SIGNIFICANT CYCLIC LOAD CONDITION. CYCLING STRESS INTENSITY RANGE IS COMPARED TO $3S_m$ LIMIT AND IS ROUGHLY PLOTTED TO ILLUSTRATE SHAKEDOWN AND THE EFFECT OF ADDING IN RESIDUAL STRESS ESTIMATE. (pp 8-10, 14)

SIGNIFICANT LOAD CYCLES ~ REF. 4, PG. F8-30.

1. HYDROSTATIC TEST — $n_1 = 132$ CYCLES
2. SUDDEN PUMP STARTUP — $n_2 = 5$ CYCLES
3. WARM-UP; COOL DOWN — $n_3 = 150$ CYCLES

STRESS RANGES AT POINT B.

1. HYDROSTATIC TEST ~ REF 4, PG. F8-19.

$\sigma_\phi = 19350$ PSI., $\sigma_\theta = 12680$ PSI, $\sigma_r = -1563$ PSI.

THESE ARE STRESSES DUE TO PRESSURE. THE ADDITIONAL BENDING AND AXIAL LOAD STRESS FROM PIPING LOADS SHOULD BE ADDED.

FROM REF. 4, PG. S8-20G:

$$\left.\begin{array}{l}\sigma_\phi = 449 \text{ DUE TO AXIAL LOAD}\\ \sigma_\phi = 7434 \text{ DUE TO BENDING}\end{array}\right\} 7883 \text{ PSI. TOTAL FOR PIPING LOADS.}$$

TO SIMPLIFY ADDING STRESSES AND FINDING STRESS INTENSITY, STRESS FROM SHEAR LOADS IS NEGLECTED HERE.

∴ TOTAL LONGITUDINAL STRESS

$$\sigma_\phi = 19350 + 7883$$
$$= 27233 \text{ PSI.}$$

USING STRENGTH REDUCTION FACTOR $K = 4$	USING $K = 5$
$S = K\sigma_\phi - (-\sigma_r)$	
$= 4(27233) + 1563 = \underline{110495}$	137728
USING ZERO STRESS CONDITION AS THE OTHER EXTREME OF CYCLIC LOAD:	
$S_r = 110495 - 0 = \underline{110495}$	137728

BY R. DEAN DATE 2/26/79 SUBJECT SHEET NO. 6 OF

CHKD. BY WJF DATE 4-16-79 JOB NO.

PARAMETER NRC-03 ORIGINAL DESIGN

1. HYDROSTATIC TEST ~ CONT.

	USING $K = 4$	USING $K = 5$
ALTERNATING STRESS (REF. 5, FIG. N-415(B)) $S_a = \frac{1}{2} S_r \frac{E_{CODE\ CURVE}}{E_{MAT'L}} = \frac{1}{2} S_r \frac{26.0}{29.3}$		
$= \frac{1}{2}(110495)(.887) =$	49025	61108
FROM FIG. N-415(B), SUMMER ADDENDA, P.3		
ALLOWABLE CYCLES: $N_1 =$	23000 cycles	9000 cycles
$\frac{n_1}{N_1} = \frac{132}{23000} =$	.006	.015

2. TRANSIENT 1, SUDDEN PUMP STARTUP:

FROM REF. 4, PG. F8-22 & F-8-23:

$\sigma_\phi = \sigma_\phi(P+LT) + \sigma_\phi(NLT)$	$\sigma_\theta = \sigma_\theta(P+LT) + \sigma_\theta(NLT)$	$\sigma_r = -p$
$= 93530 + 5541$	$= 23770 + 5541$	
$= 99071$ PSI	$= 29311$ PSI	$= -1800$ PSI.

PIPE LOAD $\sigma_\phi = 449 + 7434 = 7883$ PSI.

TOTAL $\sigma_\phi = 99071 + 7883$

$= 106954$ PSI.

	FOR $k = 4$	FOR $K = 5$
$S_r = k\sigma_\phi - \sigma_r$ $= 4(106954) + 1800$	428,816 PSI	535,770 PSI.
$S_a = \frac{1}{2} S_r \frac{26.0}{29.3}$	190,200 PSI.	237,714 PSI
N_2 FROM N415(B)	180 cycles	100 cycles
$\frac{n_2}{N_2} = \frac{5}{180}$	.028	.050

3. TRANSIENT 2, COOLDOWN:

FROM REF. 4, PG. F8-24 & F8-25:

$\sigma_\phi = \sigma_{\phi(P+LT)} + \sigma_{\phi(NLT)}$	$\sigma_\theta = \sigma_{\theta(P+LT)} + \sigma_{\theta(NLT)}$	$\sigma_r = -p$
$= 37400 + 1385$	$= 14720 + 1385$	$= -875$ PSI.
$= 38785$ PSI.	$= 16105$ PSI	
PIPE LOAD = 7883 PSI.		
TOTAL $\sigma_\phi = 38785 + 7883$		
$= 46668$ PSI.		

	USING $k = 4$	USING $K = 5$
$S = k\sigma_\phi - \sigma_r$ $= 4(46668) - (-875)$	187547	234215
USING ZERO STRESS CONDITION AS OTHER CYCLIC EXTREME: $S_r = S - 0$	187547	234215
$S_a = \frac{1}{2} S_r \frac{26.0}{29.3}$	83211	103917
N_3 FROM N-415(B)	2600 cycles	1200 cycles
$n_3/N_3 = 150/N_3$	.058	.125

CUMULATIVE USAGE FACTOR

	$k = 4$	$k = 5$
$U = \frac{n_1}{N_1} + \frac{n_2}{N_2} + \frac{n_3}{N_3}$		
$= .006 + .028 + .058$	.092	.190

BOTH RESULTS ARE WELL BELOW THE CODE MAXIMUM OF 1.0, [REF. 5, N-415.2e(b)]. ALSO, BECAUSE OF USE OF DESIGN FATIGUE CURVE N-415(B) AS REVISED, SUMMER '68 ADDENDA TO CODE, RESULTS ARE LESS THAN THE U = .515 RESULT OF ORIGINAL CALC. (REF. 4, F8-30).

STRESS COMPARISONS TO YIELD STRENGTH FOR EACH CYCLIC CONDITION AT POINT 13.

1. HYDROSTATIC TEST

a. MAX σ_ϕ = 27233 PSI. < S_y = 28100 PSI.

b. PRIMARY PLUS SECONDARY MEMBRANE PLUS BENDING STRESS INTENSITY RANGE $(P_L + P_b + Q)$ ~ NO PEAK STRESS

$S_r = [27233 - (-1563)] - 0$

$= 28796$ PSI $\leq 3S_m = 69900$ PSI.

[NOTE: $3S_m \approx 2S_y$, THEREBY ALLOWING CYCLING BETWEEN $+S_y$ AND $-S_y$.]

2. SUDDEN STARTUP (TRANSIENT 1)

a. MAX σ_ϕ = 106954 PSI. > S_y = 28100 PSI.

b. $S_r = [106954 - (-1000)] - 0$

$= 107954$ PSI. $> 3S_m = 69900$ PSI.

3. COOLDOWN (TRANSIENT 2)

a. MAX. σ_ϕ = 46668 PSI. > S_y = 28100 PSI.

b. $S_r = [46668 - (-875)] - 0$

$= 47543$ PSI. $< 3S_m = 69900$ PSI.

4. WARMUP (TRANSIENT 2)

a. MAX. $\sigma_\phi = \underset{P+LT}{15400} + \underset{NLT}{0} + \underset{PIPING}{7883} = 23283$ ~ PG. F8-20 & 21. & PAGE 5 OF THIS ATTACHMENT
$< S_y$

b. $S_r = [23283 - (-1125)] - 0$

$= 24408$ PSI. $< 3S_m$

RESIDUAL STRESS ESTIMATE

AT SAFE END, SECTION OF POINTS 13 - 14:

OUTSIDE DIA. = 11.90

INSIDE DIA. = 10.75

WALL THICKNESS = .575 IN.

FOR SCHED. 80 12" PIPE:

O.D. = 12.75

WALL THICKNESS = .687

FOR SCHED. 80 10" PIPE

O.D. = 10.75

THK. = .593

SO SAFE END SECTION IS APPROX. EQUIVALENT TO, SAY, 11" SCHED. 80 PIPE.

FROM REF 3, FIG. 6-2, FOR 11" PIPE:

$\sigma_{RESID.}/\sigma_{LOCAL\ YIELD} \approx 0.47$

$\sigma_{LOCAL\ YIELD} = S_y + .002\,E$

$= 28100 + .002\,(29.3 \times 10^6)$ AT 575°F.

≈ 86700 PSI.

SO $\sigma_{RESID.} = .47\,(86700)$

$=$ **40750 PSI**

OR FROM REF. 10, FIG. III.B.2-6:

RESID. $\sigma_\phi \approx$ **40000 PSI.** AT POINT 13 (11" PIPE).

OR FROM REF. 10, FIG. III.C.8-4 (COMPUTER ANAL. OF RESID. STRESS):

RESID. σ_ϕ = **50,000 PSI** AT POINT 13

BY R. DEAN DATE 3-2-79 SUBJECT ____ SHEET NO. 10 OF ____
CHKD BY WJF DATE 4-6-79 JOB NO. ____
PARAMETER #2C-03 ORIGINAL DESIGN

AXIAL STRESS AT POINT 13 WITH PEAK STRESS, k = 4.

TRANSIENT	σ_ϕ [PG. FB-26]	PIPING LOAD σ_ϕ [PG. 5]	TOTAL σ_ϕ	TOTAL + PEAK. $4\ \sigma_\phi$
HYDROTEST	19350	7883	27233	108932
STEADY STATE	18750	7883	26633	106532
WARMUP (TRANS 2)	15400	7883	23283	93132
COOLDOWN TRANS. 2	37400	7883	45283	181132
COOLDOWN TRANS. #1	99071	7883	106954	427816
SHUTDOWN	0	0	0	0
			PLOT PG. 14	

CYCLING SEQUENCE FOR PLOTTING (STRESSES SHOWN FOR PG. 14 PLOT).

1. START WITH YIELD STRESS DUE TO RESIDUAL STRESS FROM WELD: S_1 = 28100 + 27233 PSUEDO-ELASTIC STRESS.
2. CYCLE THRU HYDROTEST AND BACK TO SHUTDOWN } 2 TESTS MADE BEFORE INITIAL FUEL LOADING.
3. " " " " " " "

   28100 - 27233 = 867
4. CONTROLLED WARMUP TO STEADY STATE :
5. COOLDOWN #2 → WARMUP #2 → COOLDOWN #2.
   45283 - 26633 CHANGE = 18650 | 23283 - 45283 = -22000 | 45283 - 23283 = 22000
6. CONTROLLED WARMUP TO STEADY STATE : 26633 - 45283 = -18650
7. CONTROLLED SHUTDOWN : 0 - 26633 = -26633
8. CONTR. WARMUP TO ST. STATE : 26633 - 0 = 26633
9. COOLDOWN #2 → WARMUP #2 → COOLDOWN #2 (SEE #5).
10. CONTR. WARMUP TO ST. STATE : (SEE #6).
11. SUDDEN PUMP STARTUP TRANSIENT (COOLDOWN) #1 :
    106954 - 26633 = 80321
12. SUDDEN WARMUP TRANSIENT #1 : 26633 - 106954 = -80321
13. CONTROLLED SHUTDOWN : 0 - 26633 = -26633
14. CONTROLLED STARTUP : 26633 - 0 = 26633.

BY R. DEAN DATE 3-6-79 SUBJECT .... SHEET NO. 11 OF ....
CHKD. BY WJF DATE 4-16-79 JOB NO. ....
PARAMETER NCL-03 REPLACEMENT DESIGN

STRESSES IN SAFE END REPLACEMENT DESIGN

REF. 8, CBI-NUCLEAR REPORT.

OF PRIMARY CONCERN FOR COMPARISON IS POINT 130 (REF. 8, PG. 4 OF S8) WHICH CORRESPONDS IN POSITION TO POINT 13 OF THE ORIGINAL DESIGN. BOTH ARE AT THE INSIDE SURFACE OF THE SAFE END PRESSURE BOUNDARY WALL AT THE END OF THE CREVICE OR ANNULUS.

STRENGTH REDUCTION FACTOR (CONCENTRATION FACTOR) AT PT. 130:

$k = 1.7$ — REF. 8, PG. 4 OF F8 [VS. 4 IN ORIG. DESIGN]

CUMULATIVE USAGE FACTOR FOR PT. 130:

$U = .002$ — PG. 2 OF F8 [VS. 1.0 ALLOWED, VS. .09 FOR ORIG. DESIGN AT POINT 13].

STRESS INTENSITIES STRESS CATEGORY	REPLACEMENT VALUE (PSI)	REF. 8 PAGE	ALLOWABLE PSI	ORIGINAL VALUE (PSI)	REF 4 PAGE
PRIMARY MEMBRANE P_M	8898	D8-5	23300 (S_m)	15921	S8-20A
PRIM. MEMB. + BENDING $P_L + P_B$	9440	D8-29 & D8-30	14000 ($\frac{1}{2} S_Y$) PER REF. 8 34950 ($1.5 S_m$) PER CODE	18023	S8-20
PRIMARY + SECONDARY STRESS RANGE $P_L + P_B + Q$	35300	S8-5	69900 ($3 S_m$)	68626	S8-27

RESIDUAL STRESS ESTIMATE

THE FLEXIBILITY OF THE REPLACEMENT SAFE-END/THERMAL SLEEVE CONNECTION REDUCES EXPECTED RESIDUAL STRESSES TO BELOW YIELD STRENGTH.

FROM REF. 10, FIG. III. C.8-5, RESIDUAL STRESS IN THE VICINITY OF POINT 130 IS ABOUT 20,000 PSI.

AXIAL (LONGITUDINAL) TOTAL STRESS AT POINT 130 (FOR COMPARISON TO THAT AT PT. 13 OF ORIGINAL DESIGN):

FROM PG. D8 30 OF REF. 8:

$$\sigma_1 = \sigma_\phi = \underset{\text{MEMBRANE}}{28260} + \underset{\text{BENDING}}{350} = 28610 \text{ PSI. AT INSIDE (PT. 130)}$$

FROM PG. S8-23, THERMAL STRESS AT SUDDEN STARTUP TRANSIENT TIME .570 MIN.

$$\sigma_{zz} = \sigma_\phi = 11630 \text{ PSI.}$$

SO

$$\sigma_\phi (P_L + P_B + Q) = 28610 + 11630$$

$$= \underline{40240 \text{ PSI.}}$$

AS A CHECK, AXIAL STRESSES (σ_{zz}) FROM PAGES S8-29, AND S8-40 THRU -46 ARE ADDED ~

LOADING	PAGE	σ_{zz} PSI AT POINT 130
THERMAL MEMB. AND BENDING	S8-29	29216
MEMBRANE, BENDING, & PEAK*		
NOZZLE SHEAR	40	851
" MOMENT	41	5584
1000 PSI PRESSURE	42	7324
315 PSI ADDER PRESS.	43	-894
NOZZLE AXIAL LOAD	44	387
SLEEVE AXIAL LOAD	45	-722
SLEEVE SHEAR LOAD	46	-3274

TOTAL σ_{zz} = 38472 ≈ 40240 ABOVE.

EITHER FIGURE FOR AXIAL STRESS IS SOMEWHAT UNCERTAIN BECAUSE OF EXTRACTION FROM COMPUTER RESULTS OF A PROGRAM UNFAMILIAR TO THIS WRITER. ∴ USE 40000 PSI AS APPROX. VALUE.

* THIS PEAK APPEARS TO BE FROM LOCAL TEMPERATURE DIFFERENCES, SUCH AS "SKIN STRESS", AND NOT STRESS CONCENTRATION EFFECTS.

APPLYING STRESS CONCENTRATION FACTOR OF 1.7 FOR POINT 130 TO THIS APPROXIMATE TOTAL AXIAL STRESS:

$$K\sigma_{\Phi} = 1.7(40000) = \underline{68000 \text{ PSI.}}$$

THE ALTERNATING AXIAL STRESS

$$\sigma_{ALT} = 0.5(k\sigma_{\Phi}) = \underline{34000 \text{ PSI}}$$

, SOMEWHAT GREATER THAN YIELD STRENGTH OF 28100 PSI AT 575°F.

[THE COMPARABLE FIGURE FROM THE <u>ORIGINAL</u> <u>DESIGN</u>, SUDDEN STARTUP TRANSIENT, IS

$$\sigma_{ALT} = 0.5(396284) = 198,142$$

(REF. 4, PG. F8-26).]

OBVIOUSLY, THE REPLACEMENT DESIGN IS MUCH IMPROVED, AS ALSO SHOWN BY COMPARISON OF PLOTS OF CYCLIC AXIAL STRESS ON PP. 14 & 15.

BY R. DEAN DATE 3-7-79 SUBJECT DUANE ARNOLD RECIRC. NOZZLE SAFE END SHEET NO. 14 OF

CHKD. BY WJF DATE 4-16-79 JOB NO.

PARAMETER [illegible]

PLOT OF AXIAL STRESS (PRIMARY + SECONDARY) CYCLING, ORIGINAL DESIGN

STRESS LOCATION AT CREVICE ON I.D. OF SAFE END (POINT 13)

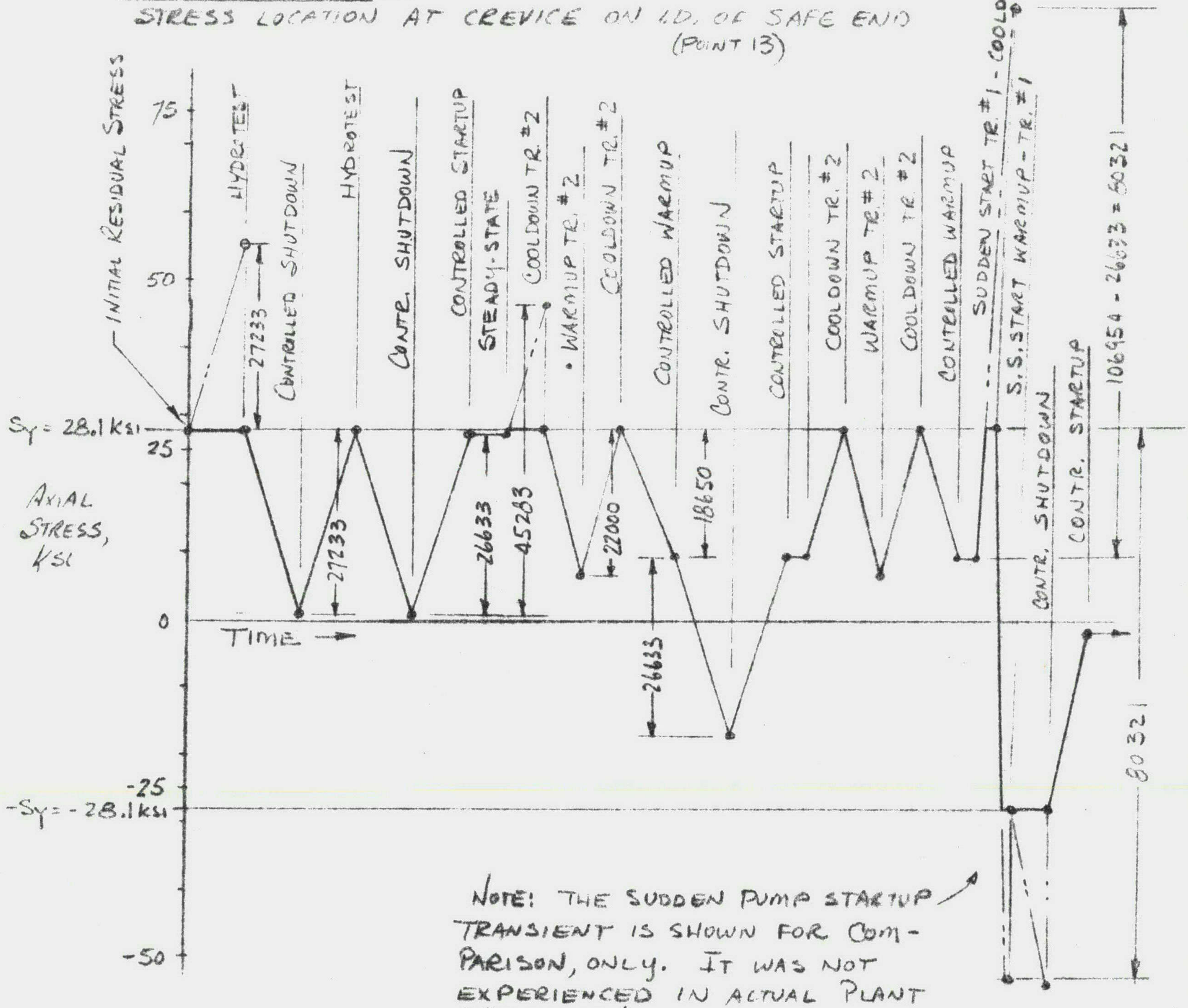

NOTE: THE SUDDEN PUMP STARTUP TRANSIENT IS SHOWN FOR COMPARISON, ONLY. IT WAS NOT EXPERIENCED IN ACTUAL PLANT OPERATION.

REFER TO PG. 10 FOR TABULATION.

BY R. DEAN DATE 3-7-79 SUBJECT SHEET NO. 15 OF 15
CHKD BY WJF DATE 4-16-79 JOB NO.
PARAMETER NKC-03

PLOT OF APPROX. AXIAL STRESS CYCLING (PRIMARY + SECONDARY)
REPLACEMENT DESIGN
STRESS LOCATION AT ANNULUS ON I.D. OF SAFE END. (POINT 130).

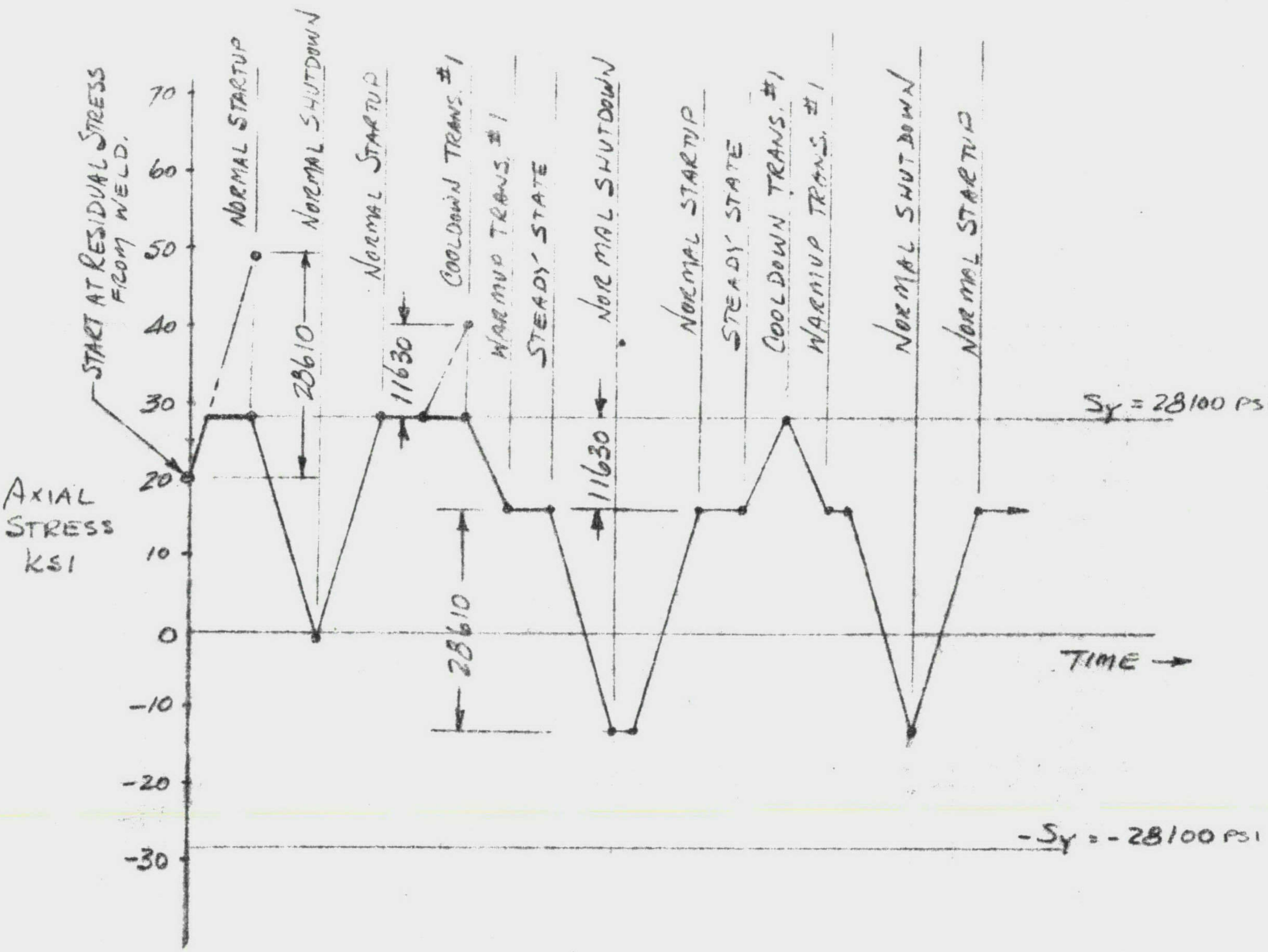

REFER TO PAGES 11 AND 12 FOR TABULATION.

BCL-585-9

FINAL REPORT

on

EXAMINATION OF INCONEL SAFE END FROM DUANE ARNOLD

to

PARAMETER INCORPORATED

January, 1979

by

V. Pasupathi, G.P. Smith, D.R. Farmelo, and J.S. Perrin

BATTELLE
Columbus Laboratories
505 King Avenue
Columbus, Ohio 43201

TABLE OF CONTENTS

LIST OF FIGURES

List of Figures (Continued)

LIST OF TABLES

1.0 INTRODUCTION

Recently Iowa Electric Light and Power Company found cracks in all of the eight Inconel safe end sections of the recirculation inlet nozzle in the Duane Arnold Plant. One of the safe ends was found to contain a visible throughwall crack. Cracks in other safe ends were detected by a combination of radiography and ultrasonic techniques. In order to determine the cause(s) of cracking Iowa Electric Light and Power Company initiated examination of the safe end section containing the throughwall crack. In parallel with this effort, examination of another safe end from Duane Arnold was initiated at Battelle's Columbus Laboratories (BCL). This parallel effort had the objective of obtaining an independent evaluation of the nature and extent of cracking.

The safe end designated as N2E was shipped to BCL and subjected to detailed nondestructive and destructive examinations including optical metallography, scanning electron microscopy, electron microprobe analysis, chemical analysis and mechanical property evaluation. This document is a final report of the data obtained in this investigation.

2.0 EXAMINATIONS AND RESULTS

2.1 Receipt of Shipment

The Inconel safe end section was received at the BCL Hot Laboratory during September, 1978. Upon opening the shipping container, the internal activity was found to be rather high, ~500-700 mRem/hr at or near the specimen. In addition the specimen was found to be highly contaminated, with smearable activity being 900,000 dpm.

2.2 Visual Examination

A visual examination of the sample was made using a magnifying glass. Care was taken not to disturb the deposits on the specimen surface. The outer surface of the specimen was relatively clean with azimuthal orientation marks 0-20 around the circumference of the safe end. These markings had been made with a felt tip marker and corresponded to the locations of radiography films.

In addition to these marks, the piece also contained a hose clamp containing the specimen identification number plate showing N2E. The location of the repair weld could be clearly seen on the outer surface. The inner surface of the specimen had a rust colored coating of loose powder. This powder could be easily scraped off. Careful examination of the inner surface failed to reveal any cracks. The as-received condition of the specimen was documented by photography in detail. Figures 1a and 1b show the appearance of the specimen.

2.3 Dimensional Measurements

Dimensional measurements made on the specimen consisted of wall thickness and diameter measurements. Wall thickness measurements were made using a micrometer. Location of the measurements and the results are shown in Table 1. Diameter measurements were made from photographs taken during visual examination. The outer diameter at the large end was 14.00 in. and that at the smaller end was 11.3 in.

2.4 Destructive Examinations

2.4.1 Specimen Sectioning. The specimen was marked for sectioning according to the cutting diagram supplied by Parameter Incorporated. Five thin samples were cut with a band saw. Locations of the samples are shown in Figure 2. Figure 3 shows the samples cut from the safe end.

Sample No. 1 - At radiography location 5
Sample No. 2 - Between radiography location 4 and 5
Sample No. 3 - Between radiography location 3 and 4
Sample No. 4 - Between radiography location 14 and 15
Sample No. 5 - Between samples 1 and 2.

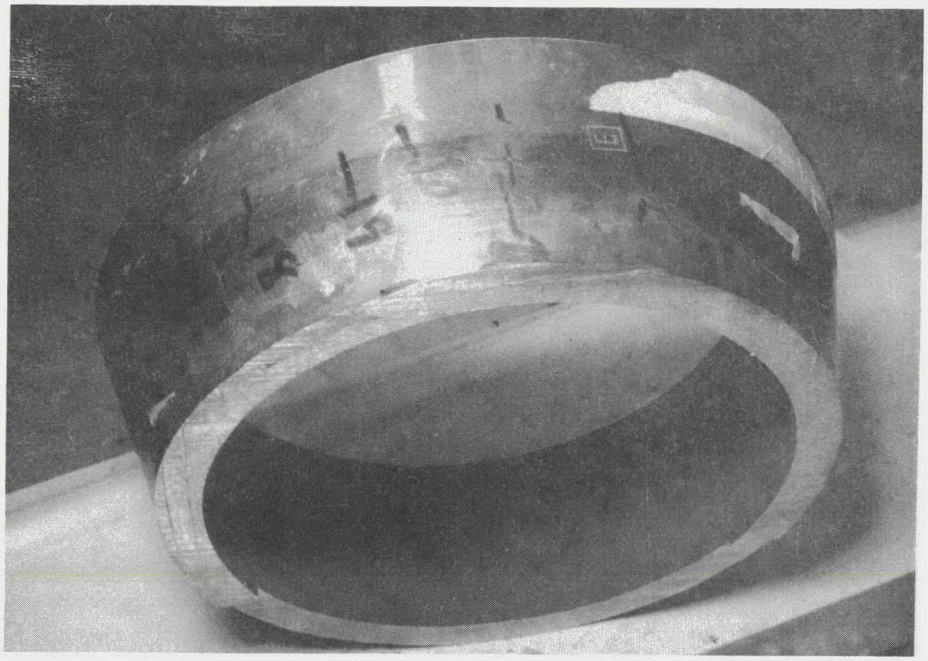

(a)

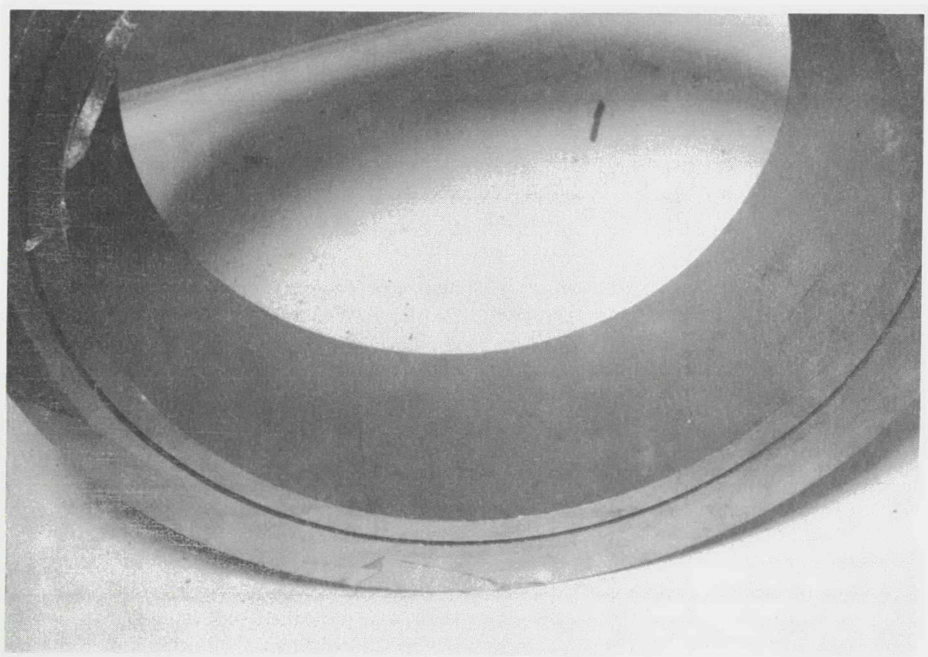

(b)

FIGURE 1. APPEARANCE OF DUANE ARNOLD INCONEL SAFE END IN THE AS-RECEIVED CONDITION

TABLE 1. RESULTS OF WALL THICKNESS MEASUREMENTS

Sector (Orientation)	Locations 1	2	3	4
0 (0°)	1.4688"	1.3065"	0.8642"	0.7515"
3 (45°)	1.4850"	1.3030"	0.8610"	0.7450"
5 (90°)	1.4862"	1.2988"	0.8592"	0.7380"
8 (135°)	1.4802"	1.3018"	0.8650"	0.7215"
10 (180°)	1.5112"	1.3015"	0.8565"	0.7142"
13 (225°)	1.4715"	1.3038"	0.8420"	0.7190"
15 (270°)	1.4608"	1.3085"	0.8452"	0.7238"
18 (315°)	1.4565"	1.3090"	0.8650"	0.7322"

SCHEMATIC OF SAFE END CROSS SECTION INDICATING
LOCATIONS OF WALL THICKNESS MEASUREMENTS

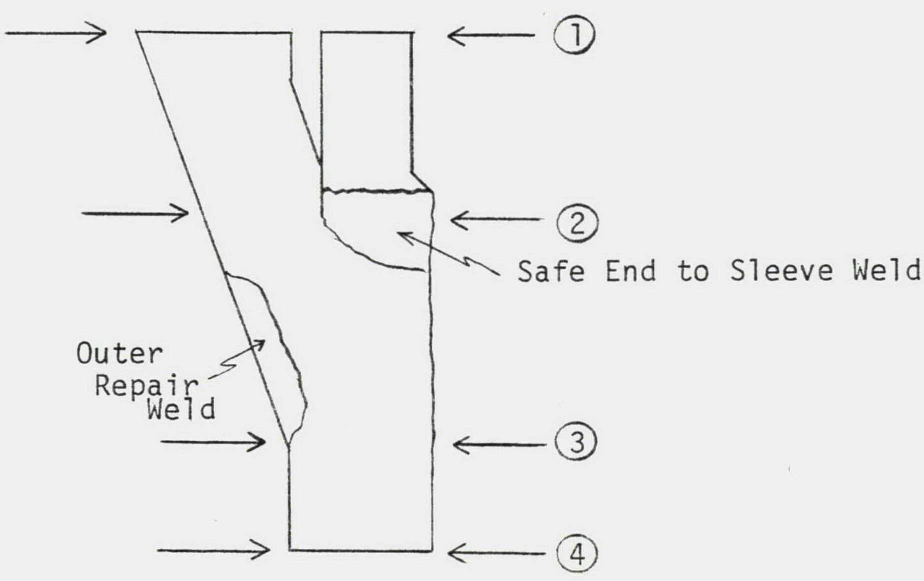

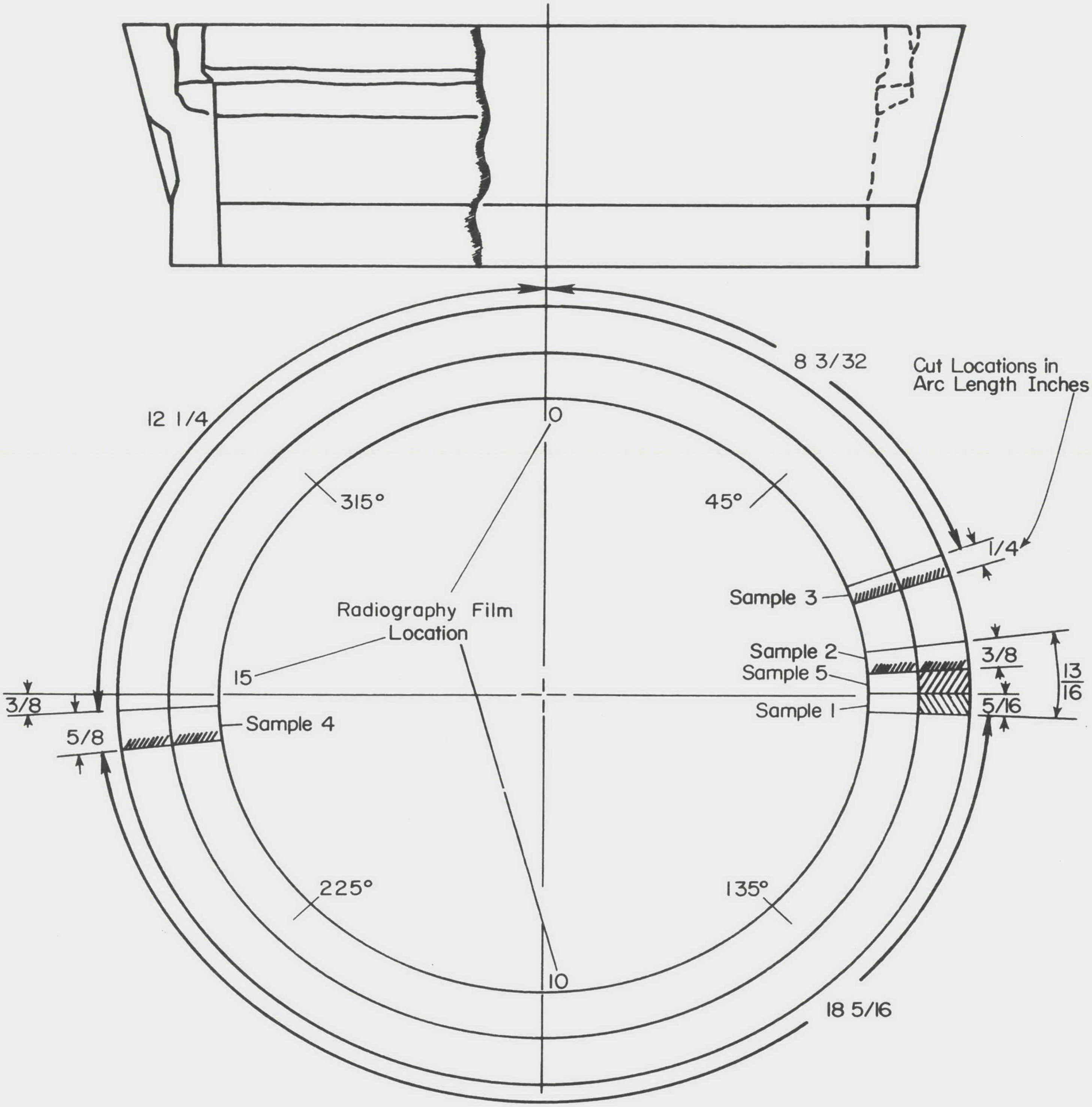

FIGURE 2. LOCATION OF METALLOGRAPHIC AND SEM SPECIMENS ON DUANE ARNOLD SAFE END N2-E

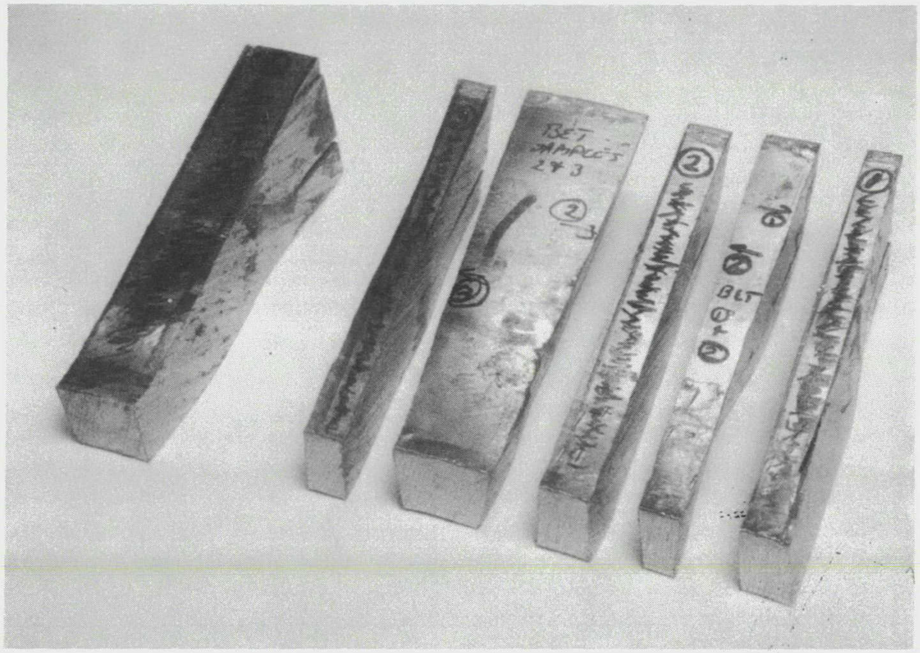

(a)

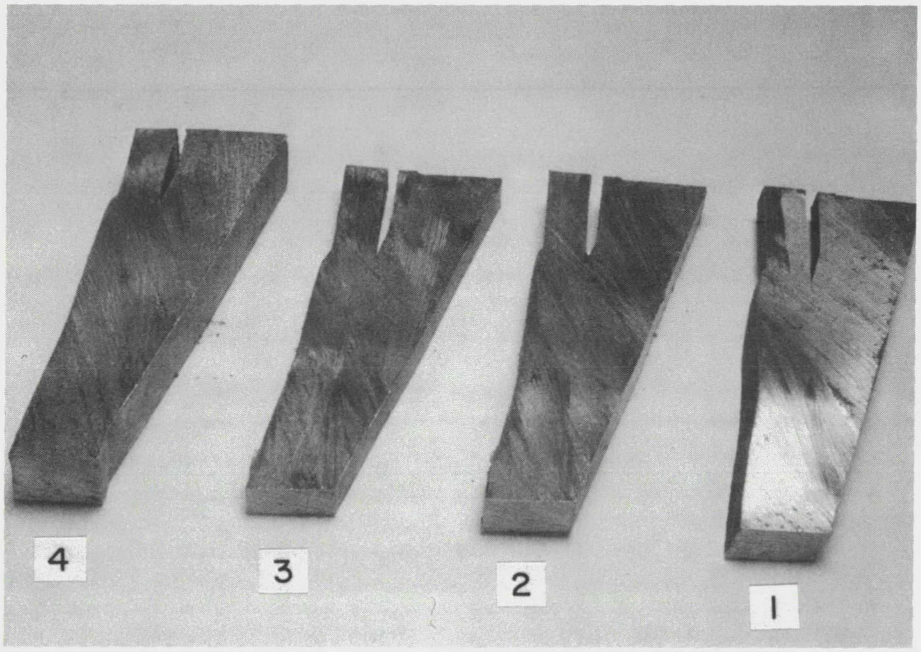

(b)

FIGURE 3. CONDITION OF SAMPLES AFTER BEING CUT FROM SAFE END

Prior to making the first cut, small indentations were made with a center punch on either side of the first cut location. The distances between these marks were measured. Three such pairs of indentations were made and the distances measured.

While the first cut for Sample No. 1 was being made, it was found that the cut closed tightly and the band saw blade could not be pulled out. The frame was removed and the blade was left in the cut. A new blade was inserted and the second cut made. After completing this cut the sample had to be pried loose. The distance between the centerpunch marks was measured after the sample was cut out. The measurements obtained before and after are shown in Figure 4. Also shown are the locations of the marks.

2.4.2 Metallographic Examination. Samples 2, 3, and 4 were mounted in epoxy resin and prepared for metallographic examination. The samples were milled to obtain a flat surface and ground with silicon carbide papers of grit 120 through 600. They were then polished with a slurry of Linde A alumina. Samples 2 and 4 were examined in the as-polished condition and Sample 3 was etched electrolytically with a 10 percent solution of oxalic acid.

All three samples contained cracks. The cracks were all intergranular in nature. In all samples, the initiation site of cracks was in the region of tight crevice between the sleeve and the safe end and radiated outward. The length of the tight crevice was found to be in the range 0.2-0.3 in. and the width was 0.002-0.005 in. No cracks were observed in the sleeve. In Samples 2 and 4 some grey areas were observed adjacent to tight branches of the cracks. These areas appeared to be of different composition. Similar areas were also observed along "tunnels" radiating from the cracks. The source of this grey phase area is not known.

The crack did not penetrate through the cross section of the safe end in any of the samples examined. In Samples 2 and 3 the crack had penetrated approximately 80% of the wall. In Sample 4, which was obtained

Location of Center Punch Marks

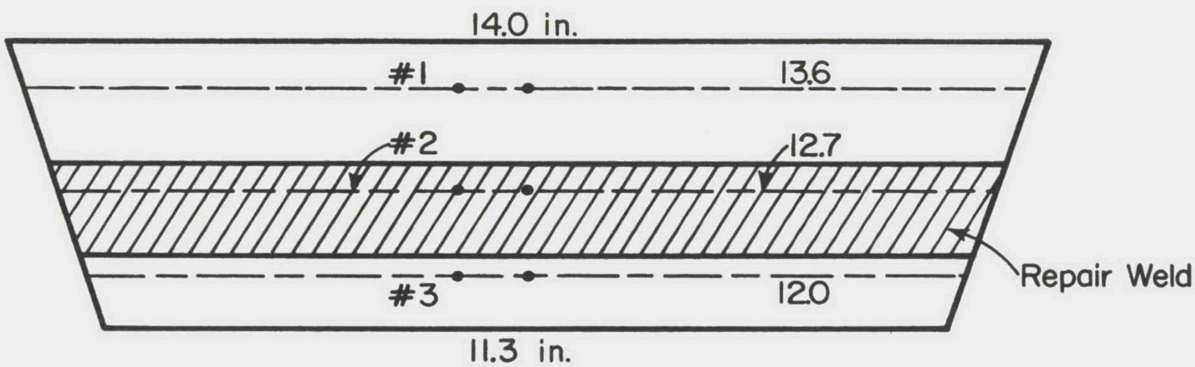

Distance Between Punch Marks Inches

	Before Cut	After Cut	Change
No. 1	0.9230	0.8754	0.0476
No. 2	1.0220	0.9250	0.0970
No. 3	0.9650	0.8800	0.085

FIGURE 4. CHANGE IN OUTER CIRCUMFERENCE DURING SECTIONING OF DUANE ARNOLD SAFE END

from the opposite quadrant, the crack penetration was about 30%. The crack characteristics were documented by photography. Figures 5 and 6 show the results from Samples 2 and 4, respectively.

Sample 3 was examined in detail to characterize the microstructure of various parts of the sample. Figure 7 shows the results. The photomicrographs show that no major abnormalities are apparent in the microstructure of the safe end with the exception of sensitization near the sleeve to safe end weld. However, it appears that the thermal sleeve is sensitized (as evident from carbides precipitated at grain boundaries) rather uniformly even away from the weld.

Sample 3 was subsequently reprepared and etched with a mixture of 20 ml H_2O, 20 ml HNO_3, and 80 ml HCl. The purpose of this procedure was to clearly identify the location of the crack with respect to the weld and heat affected region. With this technique, the crack initiation site was found to be in the re-solution treated region of the heat affected zone. Figures 8 through 10 show details of the crack location and crack characteristics.

In order to further characterize the extent of sensitization of the safe end in the vicinity of the crack, sample 4 was repolished and electrolytically etched with 10% Nital. This procedure is expected to show grain structure in the material regardless of the degree of sensitization. After examination, the sample was repolished and etched electrolytically with a 15% solution of phosphoric acid. This etching process preferentially attacks carbides in the grain boundaries and the matrix. Figure 11 shows a comparison of the microstructure at the crack initiation site with the two etching procedures. Examination of the photomicrographs shows that the sensitized region in the safe end is rather narrow and that the crack initiation site is located in the re-solution treated region adjacent to the weld. The thermal sleeve also appears to be sensitized to a greater extent in comparison to the safe end.

Additional experiments were carried out on sample 4 using modified glyceregia as the etchant. The etching solution consisted of 10 ml HNO_3, 10 ml acetic acid, 20 ml HCl and 30 ml glycerine. This process was expected to delineate chromium depleted regions along grain boundaries.(1)

---

(1) References at end of text.

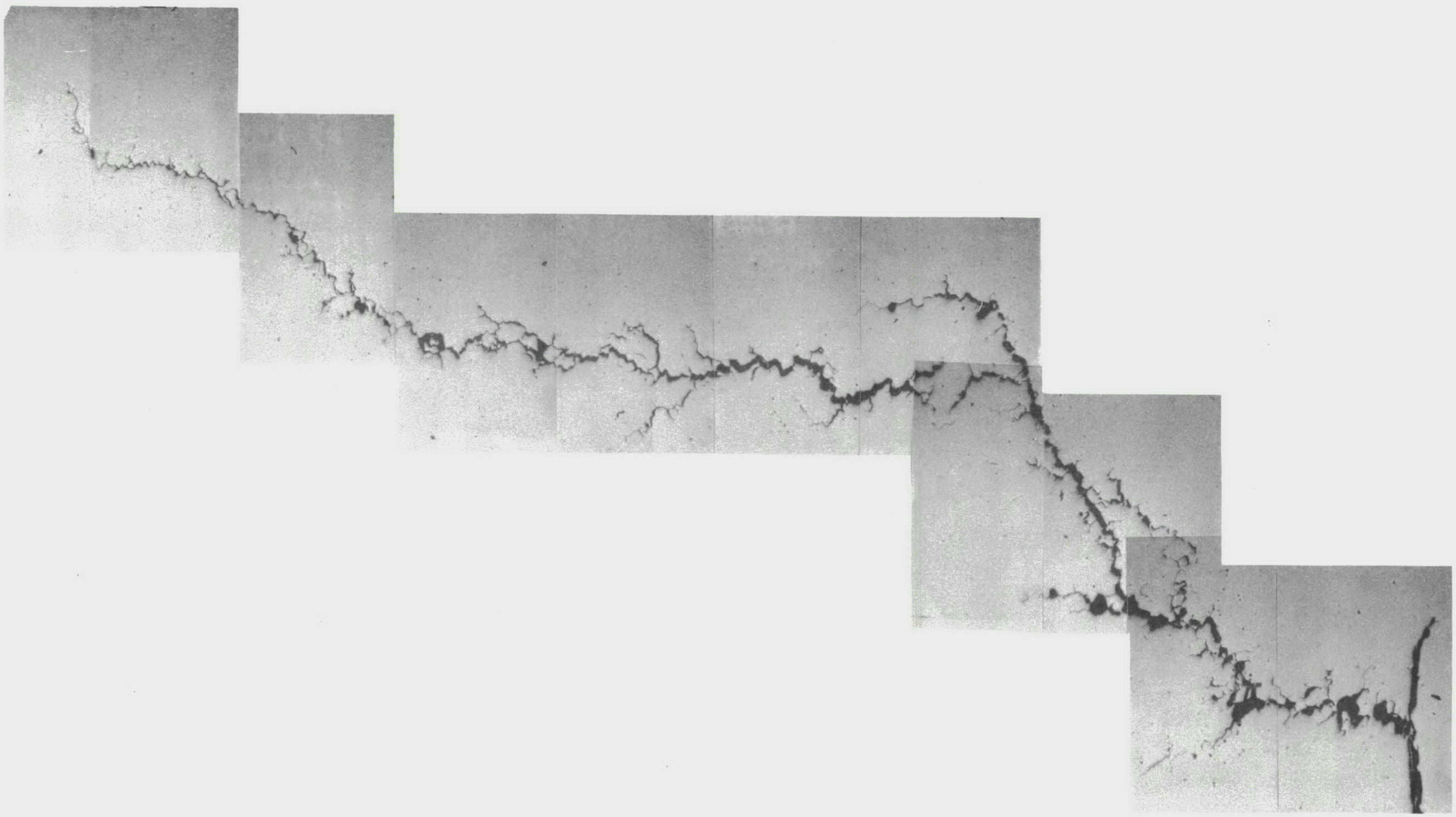

Crevice

FIGURE 5. MICROGRAPH MONTAGE OF CRACK IN SAMPLE 2

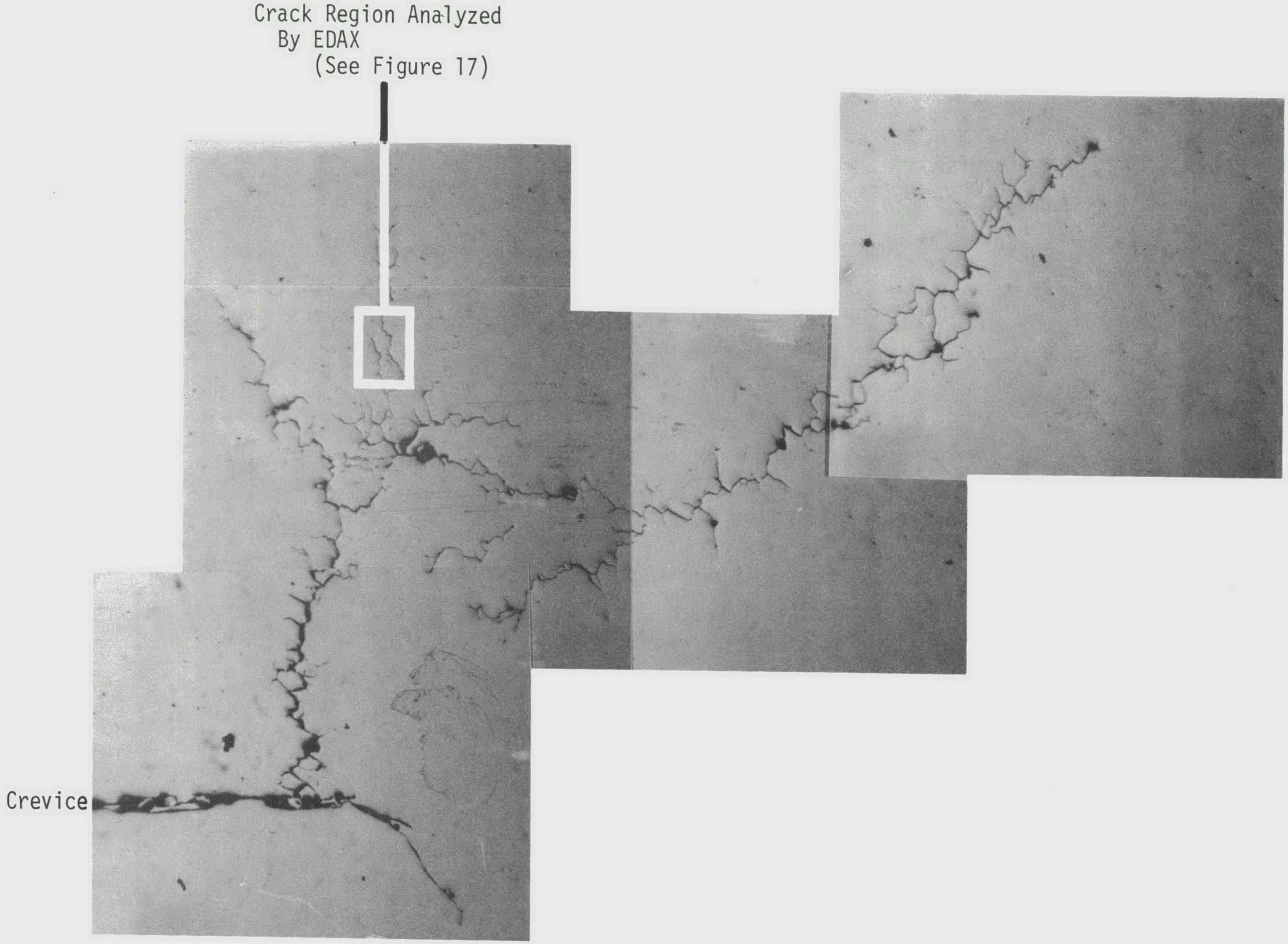

FIGURE 6. MICROGRAPH MONTAGE OF CRACK IN SAMPLE 4

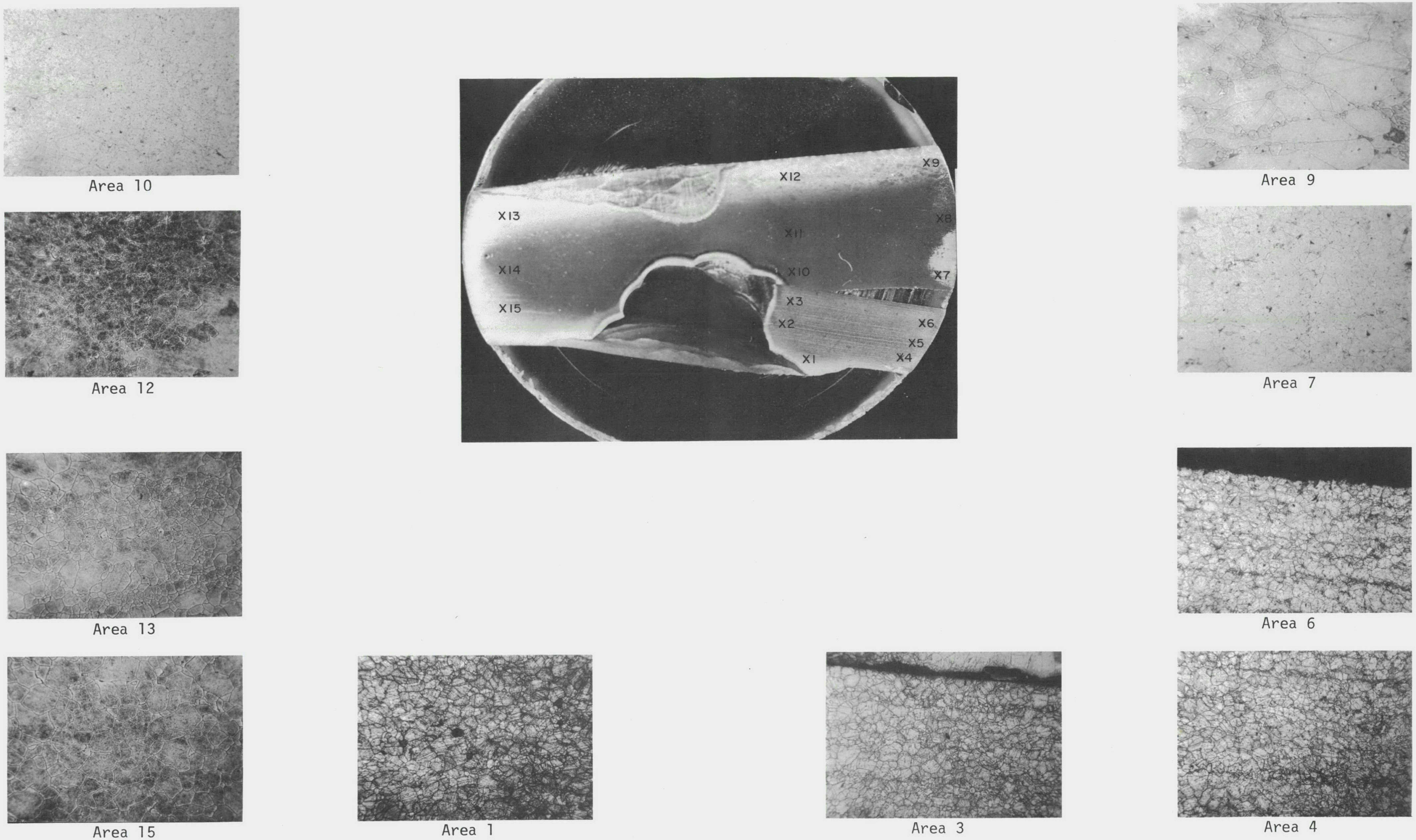

FIGURE 7. TYPICAL MICROSTRUCTURES AT VARIOUS LOCATIONS OF SAMPLE 3 CROSS SECTION

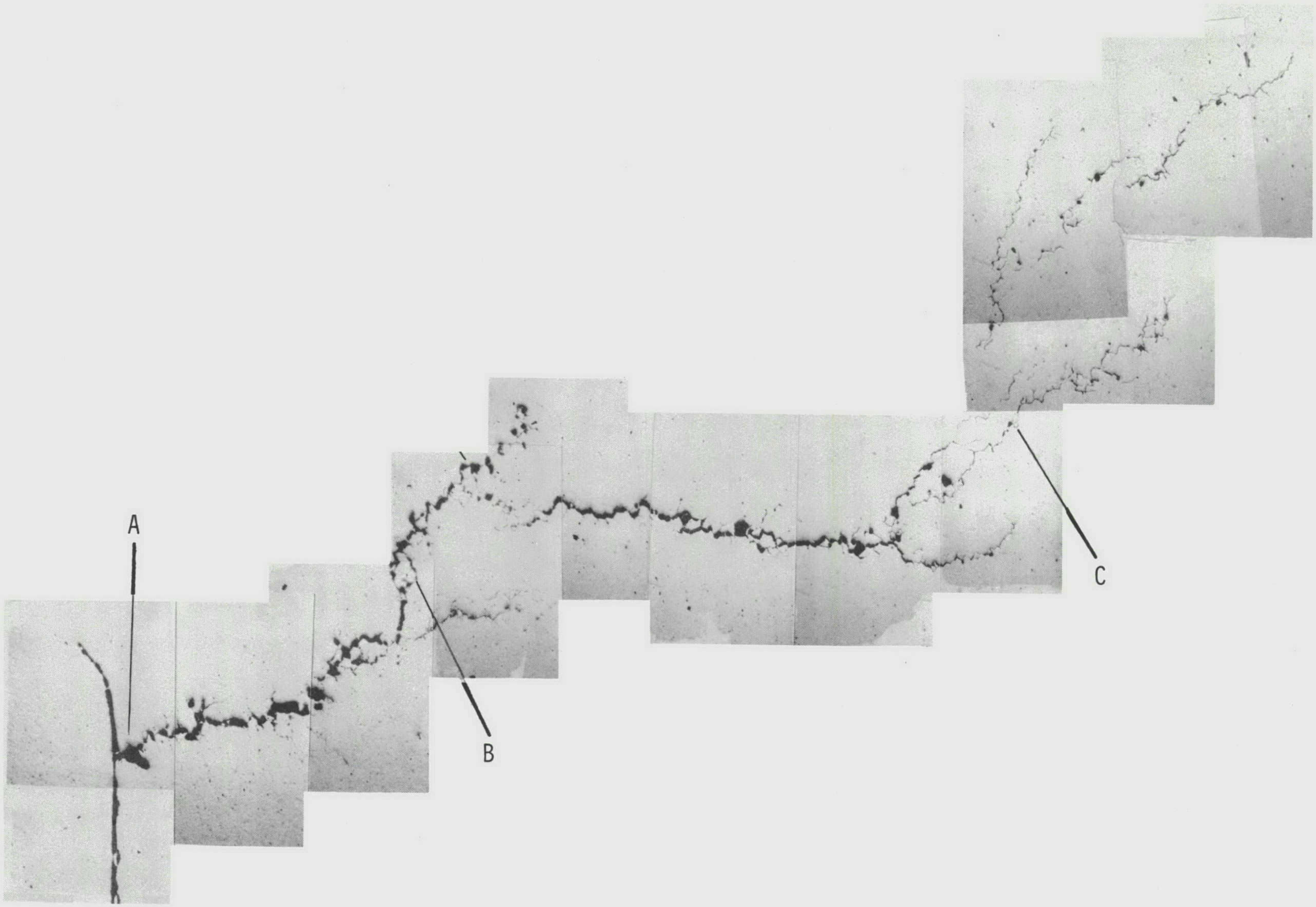

FIGURE 8. MICROGRAPH MONTAGE OF CRACK IN SAMPLE 3 AFTER ETCHING

Details of areas labeled A, B, and C are presented at higher magnification in Figures 9 and 10.

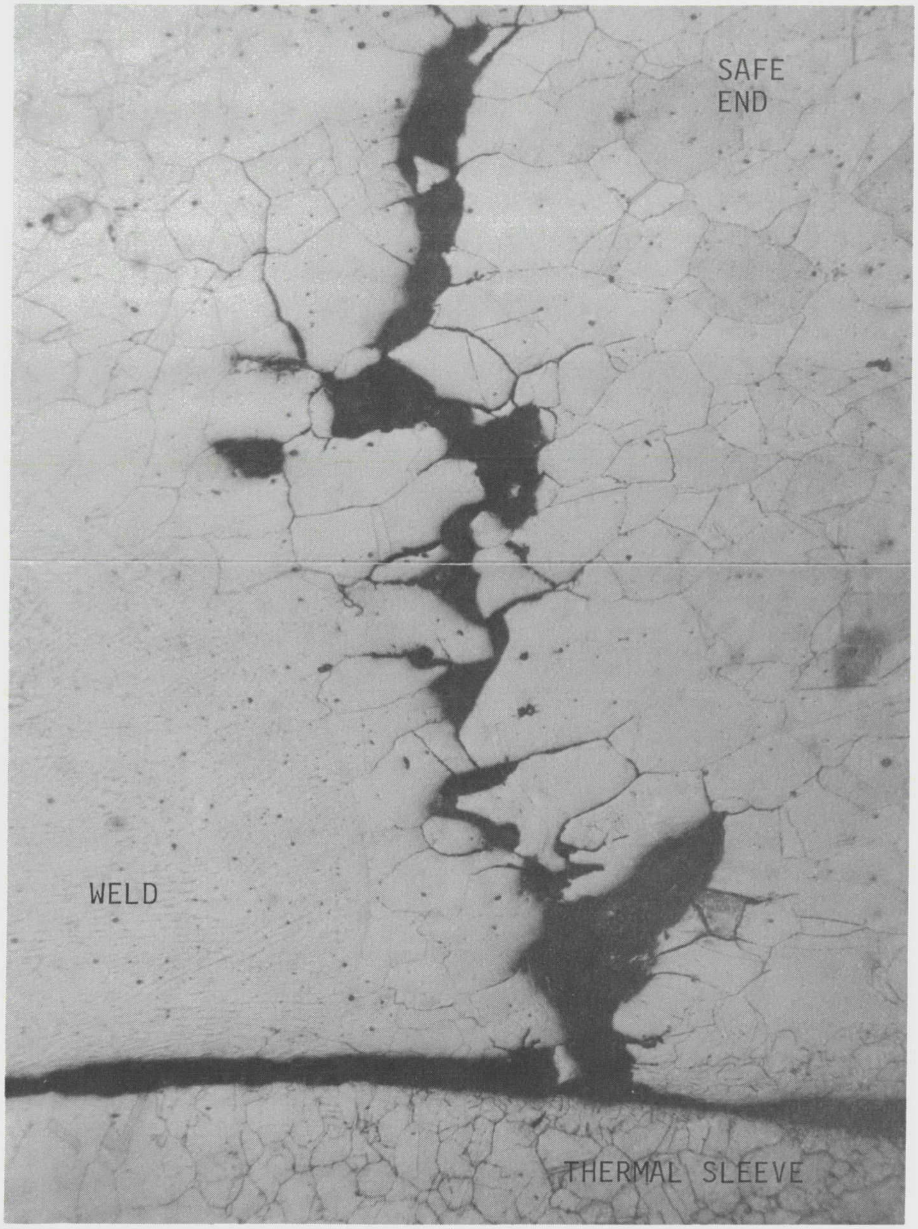

FIGURE 9. MICROGRAPH OF AREA A ON FIGURE 8
FROM ETCHED SAMPLE 3

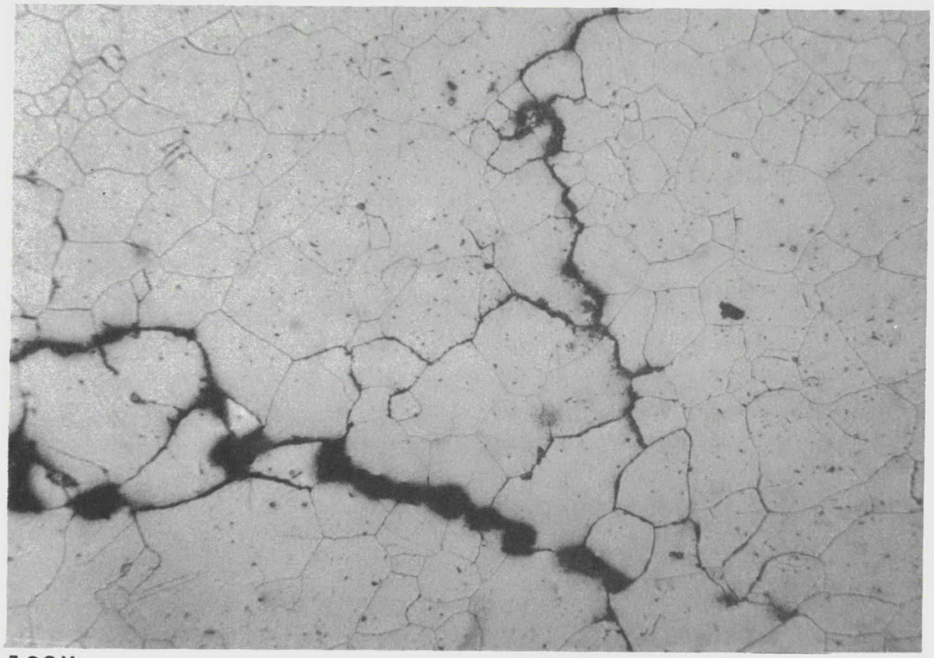

100X

(B)

100X

(C)

FIGURE 10. MICROGRAPHS OF AREAS B AND C FROM FIGURE 8
FROM ETCHED SAMPLE 3

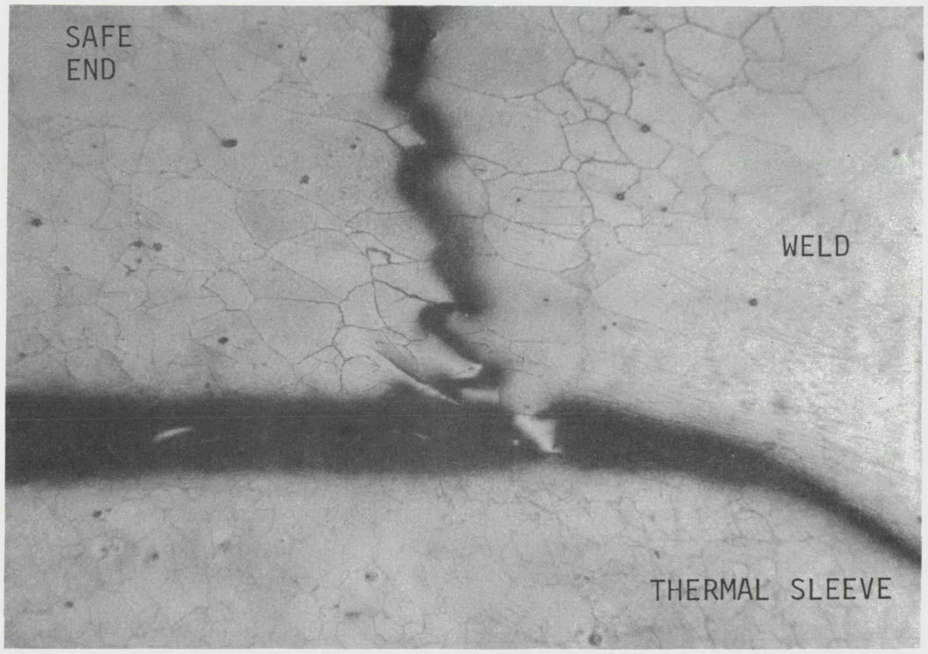

100X

19% Nital Etch

(a)

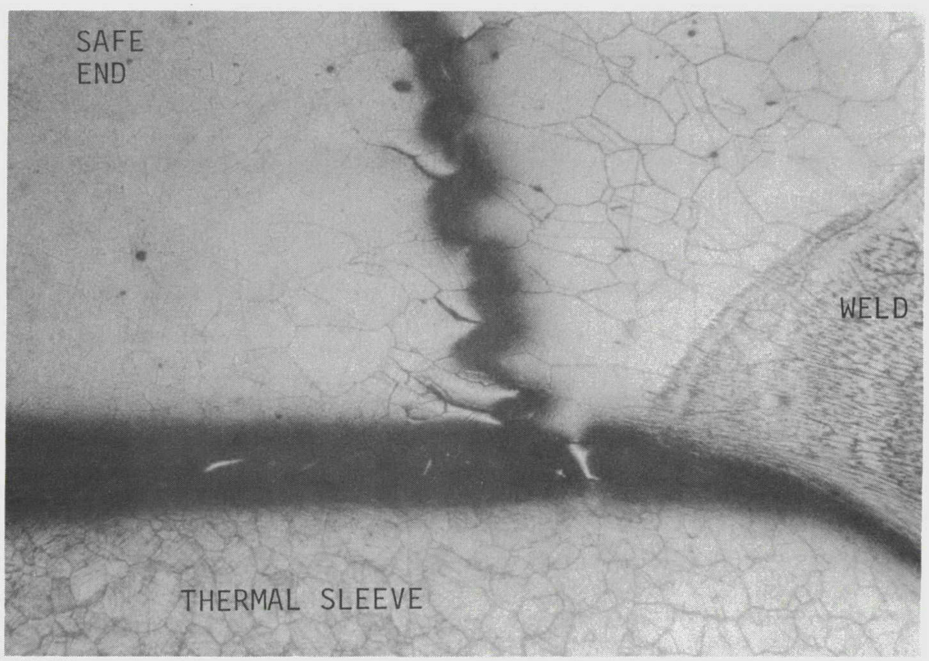

100X

Phosphoric Acid Etch

(b)

FIGURE 11. MICROSTRUCTURE OF THE CRACK INITIATION SITE IN SAMPLE 4

Examination of the specimens showed extremely narrow and barely discernible regions (probably chromium depleted areas) in the relief adjacent to the grain boundaries in the heat affected region. Initially, it was planned to analyze this region using the scanning electron microscope to determine if the composition was different from the grain matrix. This plan was abandoned because of the difficulty in discerning these regions. The etching procedure, however, was found to define more clearly areas previously identified as grey phase. Figure 12 shows one such area in the sample.

2.5 Tensile Tests

From the remaining parts of the Inconel safe end a large piece was sectioned so that specimens for tensile tests could be machined. The large piece was cut between radiography locations 0 and 4 as shown in Figure 13. The cut piece was decontaminated and ultrasonically cleaned and five tensile test specimens were machined. Figure 14 shows schematically the location of the specimens in the safe end and Figure 15 shows the dimensions of the tensile specimens used.

The specimens were tested at room temperature. The results obtained are shown in Table 2. From the results presented in Table 2, it is clear that no degradation of the Inconel safe end tensile properties was observed.

2.6 Chemical Analyses

2.6.1 Tests of pH in Crevice. Tests to determine the pH of the residue in the crevice were carried out using deionized water and litmus paper. Although litmus changes indicated pH to be in the 4-6 range, such reactions were variable and not sufficiently positive to enable conclusive determination of the acidity of corrosion products.

2.6.2 Liquid Samples From Crevice. The section cut from the pipe for tensile test samples was used to obtain samples for chemical analysis. Prior to decontamination the crevice area was rinsed with distilled water and the rinse solution was collected and analyzed by emission spectroscopy. This procedure involves evaporating the water and analyzing the residue. The major element in the residue was found to be Na. Trace amounts of Mn, Si, Cu, Ni, Cr, Ti, Al, B, Fe, Mg, K, Ca, Ba, and Sr were also detected.

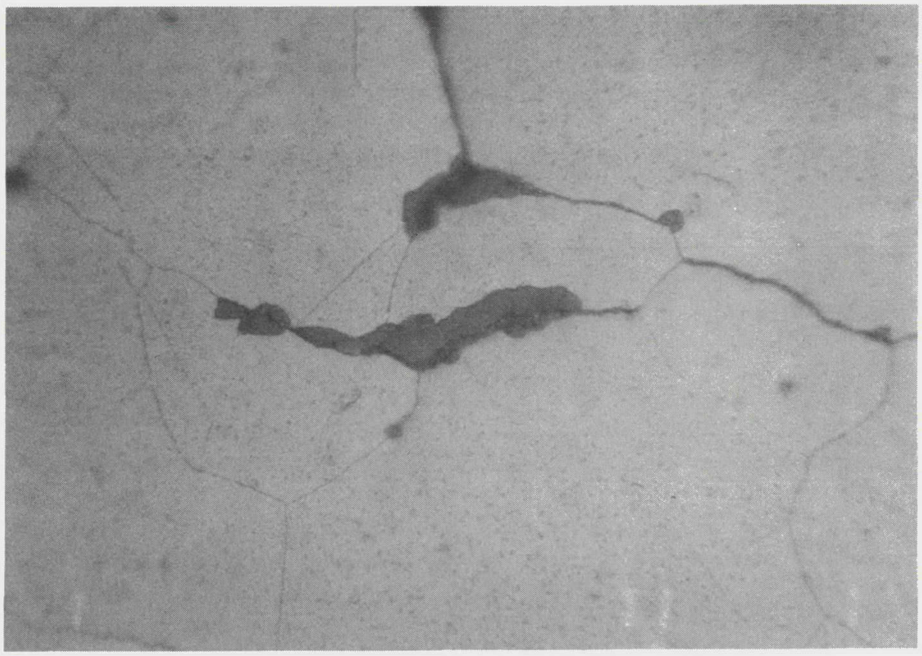

500X

FIGURE 12. APPEARANCE OF THE GREY PHASE ADJACENT TO A TIGHT CRACK BRANCH

Sample was etched with aqua regia glycerine and acetic acid mixture to reveal chromium depleted regions.

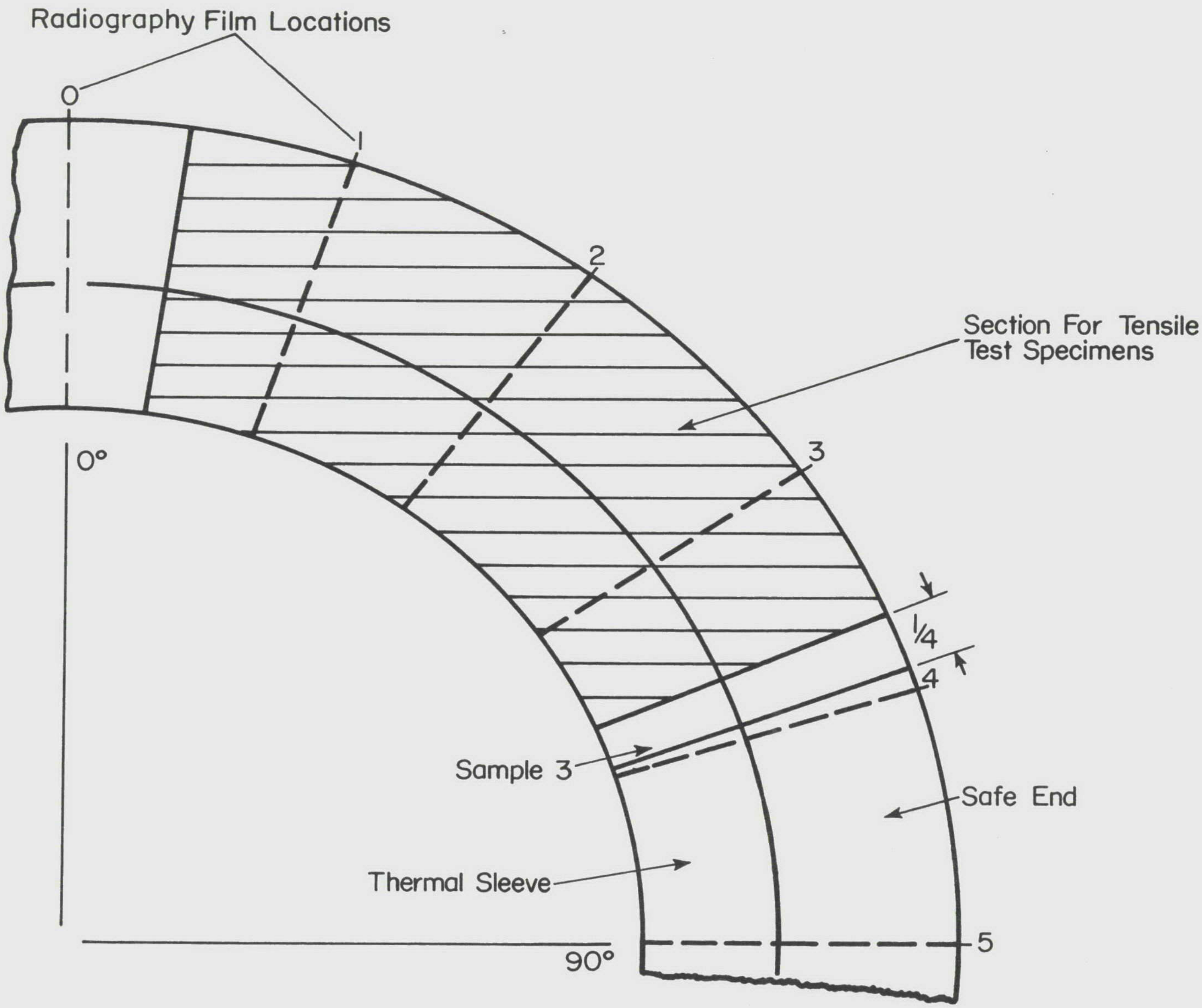

FIGURE 13. LOCATION OF THE SECTION FROM WHICH TENSILE TEST SPECIMENS WERE MACHINED

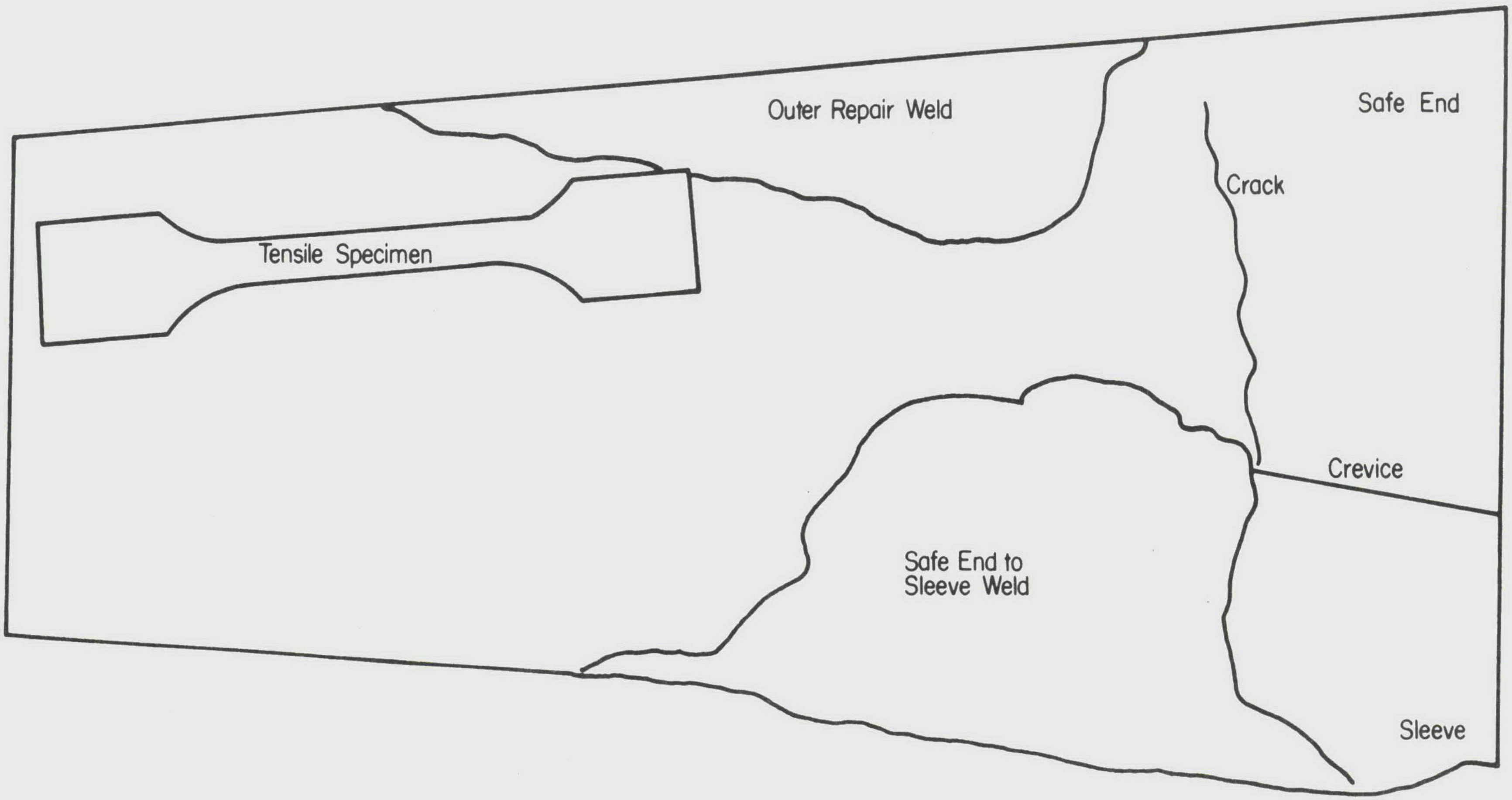

FIGURE 14. SCHEMATIC DIAGRAM INDICATING LOCATION OF TENSILE TEST SPECIMENS MACHINED FROM SAFE END

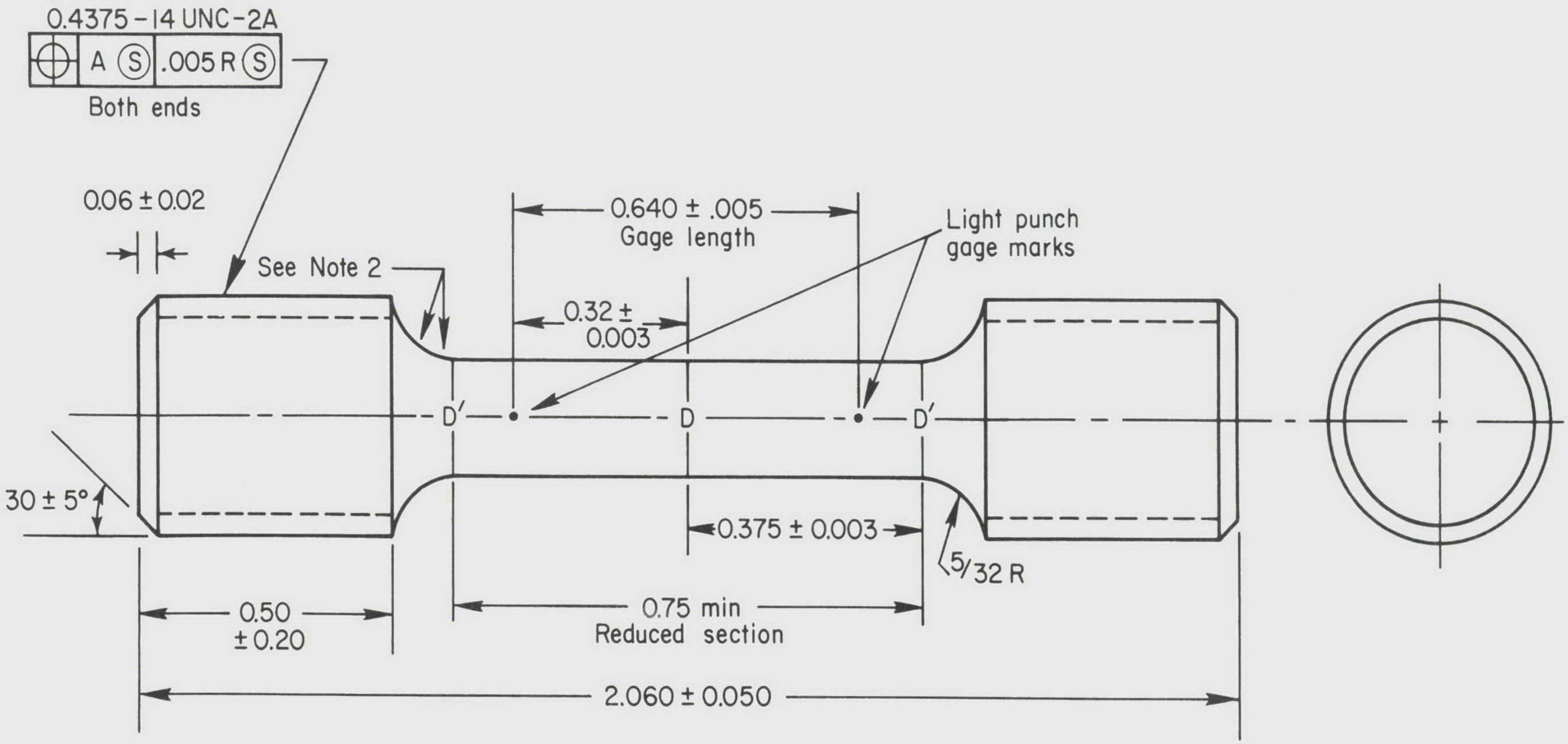

Notes: 1. D = 0.160 ± 0.001 diameter at center of reduced section. D' = actual D + 0.002 to 0.003 at ends of reduced section tapering to D at center.

2. Grind reduced section and radii to 32√ radii to be tangent to reduced section with no circular tool marks at point of tangency or within reduced section. Point of tangency shall not lie within reduced section.

FIGURE 15. TENSILE TEST SPECIMEN DIMENSIONS

TABLE 2. RESULTS OF ROOM TEMPERATURE TENSILE TESTS FOR DUANE ARNOLD INCONEL SAFE END MATERIAL

Test Specimen No.	Yield Strength (ksi)	UTS (ksi)	Percent Total Elongation (in 0.640 in.)	Percent Reduction in Area
DA-1	47.5	107.0	41.9	57.8
DA-2	48.0	106.0	40.15	57.5
DA-3	46.8	105.7	39.5	58.2
DA-4	48.8	104.5	38.3	61.0
DA-5	49.3	107.0	40.6	58.7
Precharacterized* Material	44.0	100.0	38.0	53.0

*Results of Precharacterized Testing obtained from Chicago Bridge and Iron Company Nozzle Certified Test Reports. Specimen gage length for Precharacterized Testing - 2.0 in.

2.6.3 Corrosion Deposits on the Inner Surface of Specimens. The red powdery deposit observed on the inner surface was scraped off and collected. This sample was analyzed using an X-ray diffraction technique. The major portion of the scrapings (60-70%) was found to be hematite (Fe_2O_3). The remainder could not be identified.

2.6.4 Bulk Metal Analysis. Chemical analysis of a bulk metal sample (from safe end) was carried out. The samples consisted of a metal chunk and fine chips. The results, shown in Table 3, indicate that the composition of the material was within the limits of specification.

2.7 Scanning Electron Microscopy

Four safe end specimens, each containing a partial thruwall crack, were examined by scanning electron microscopy (SEM). Two samples (Sample Nos. 2 and 4) were mounted and metallographically polished prior to SEM examination as stated in Section 2.4.2. The remaining SEM samples, identified as Sample Nos. 1 and 5 were examined along the fracture surface. Figure 2 identifies the location and the surfaces examined of each safe end sample.

2.7.1 Polished Samples, SEM Examinations. SEM examination and Energy Dispersive X-Ray Analysis (EDAX) of the fractures and fracture areas of Samples 2 and 4 provided several interesting results. As can be seen from Figures 5 and 6, the cracks observed in both samples contain numerous branches or tributaries. In addition, the cracks appear to originate in the weld heat affected zone at the crevice between the safe end and the thermal sleeve.

SEM examination of many of the tight crack tributaries in Samples 2 and 4 indicated that a phase different from the Inconel base metal was present directly adjacent to the crack. A typical SEM micrograph of this phase with its corresponding X-ray spectrum is presented in Figure 16. EDAX analysis indicated that this grey phase was chromium rich. The chromium enhancement of the grey phase was determined to be approximately 60-80% relative to the base metal material. In addition to the composition variation of the grey phase, numerous instances, of what appears to be transgranular tunneling (shown in Figure 16) were observed in areas where grey phase was found.

TABLE 3. CHEMICAL ANALYSIS OF INCONEL SAFE END BULK METAL MATERIAL

Element	Percent
Ni	73.6
Cr	15.6
Fe	7.8
Al	0.4
Ti	0.3
Mn	0.2
Si	0.2
Cu	0.1
Mo	0.1
S	0.002
Si	0.3
P	0.03

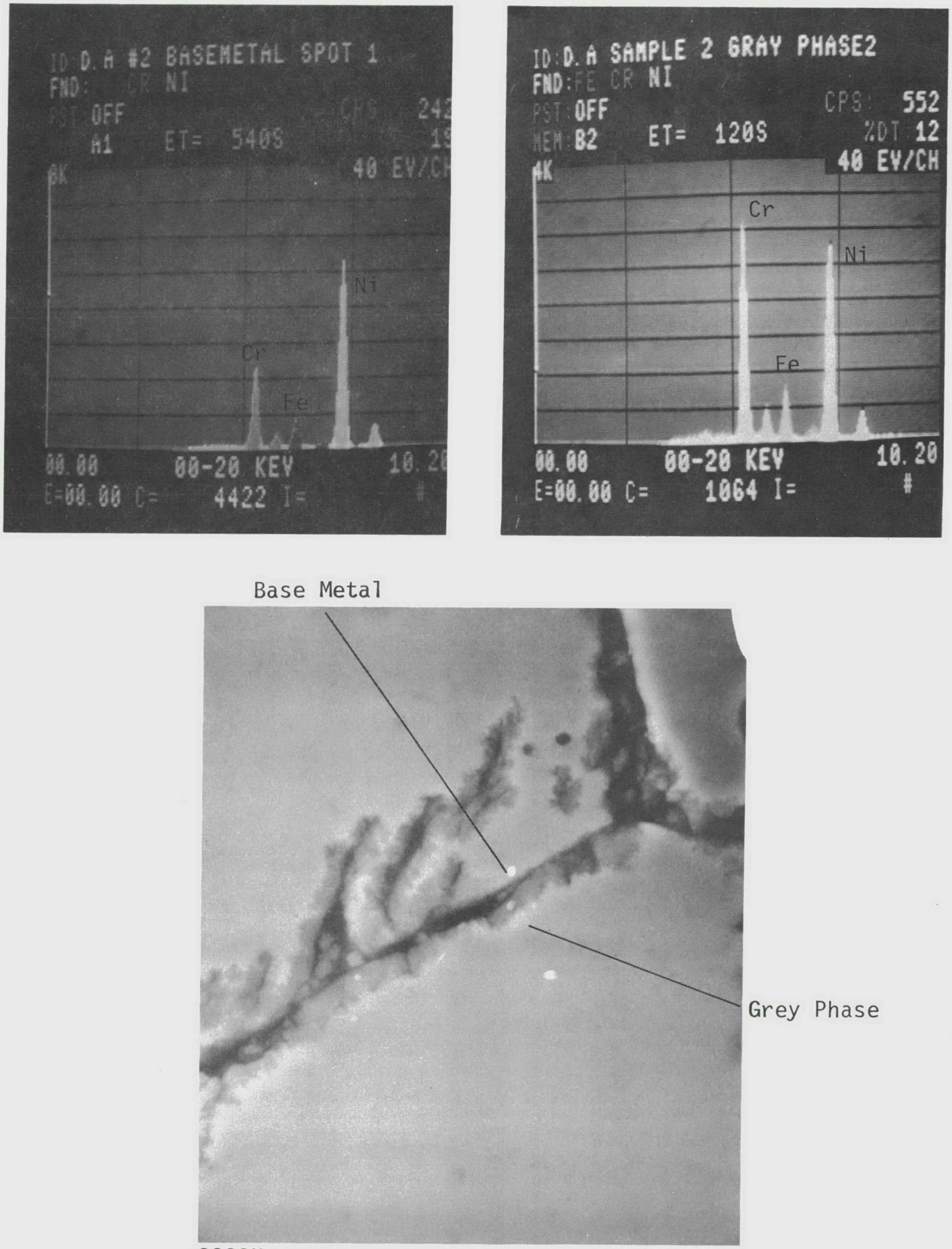

FIGURE 16. SEM MICROGRAPH OF GREY PHASE AND CORRESPONDING EDAX ANALYSES OF BASE METAL AND GREY PHASE

EDAX analysis of material observed within the crack both adjacent to the grey phase and in areas where no grey phase is found indicate an iron rich material relative to base metal compositions. Figures 17 and 18 present SEM micrographs and EDAX spot analysis performed well within the crack and at the crevice on Sample No. 4. As can be seen in Figure 17 the EDAX analysis of material within the crack indicates excessive iron relative to base metal analysis. However, no iron depletion can be observed in the material adjacent to the crack. EDAX analysis performed on material within the crevice (Figure 18) at a location near the crack origin indicate similar iron rich material. Comparison of the two relative iron contents from EDAX analysis at the crevice with analysis in the crack indicate a significantly higher iron content of material well within the crack.

Numerous titanium inclusions were observed throughout the base metal on Samples 2 and 4. A typical titanium inclusion observed in Sample 4 is illustrated by SEM micrograph in Figure 19 in conjunction with its X-ray spectrum.

2.7.2 SEM Fractography. As stated previously, safe end Sample No. 5 was examined by SEM. Figure 20 presents a schematic of Sample No. 5 showing the fracture surface examined. In order to expose the fracture surface for examination the specimen was mechanically fractured. Figure 21 presents a photomacrograph of the fracture surface examined. The bright material to the left is the region of uncracked safe end wall thickness which was mechanically fractured. Examination of this region following fracture indicated the material to be ductile.

Detailed SEM examination was performed on the entire fracture surface. Figure 22 presents SEM fractograph montages at the beginning (near crevice) middle, and tip of the crack along the fracture surface. The mode of cracking, as indicated by the SEM fractographs, was intergranular fracture.

Numerous EDAX analyses were performed on several areas of the fracture and crevice. Figures 23, 24, and 25 present SEM fractographs illustrating typical areas chosen for EDAX analysis (i.e., Figures 23b, 24a, and 25b present actual areas examined by X-ray near the crevice, in the middle and at the tip of the fracture, respectively). In addition, Figure 24b presents a SEM micrograph of a grain facet (from Figure 24a) showing a network of needle-like corrosion products on which a spot EDAX analysis was performed.

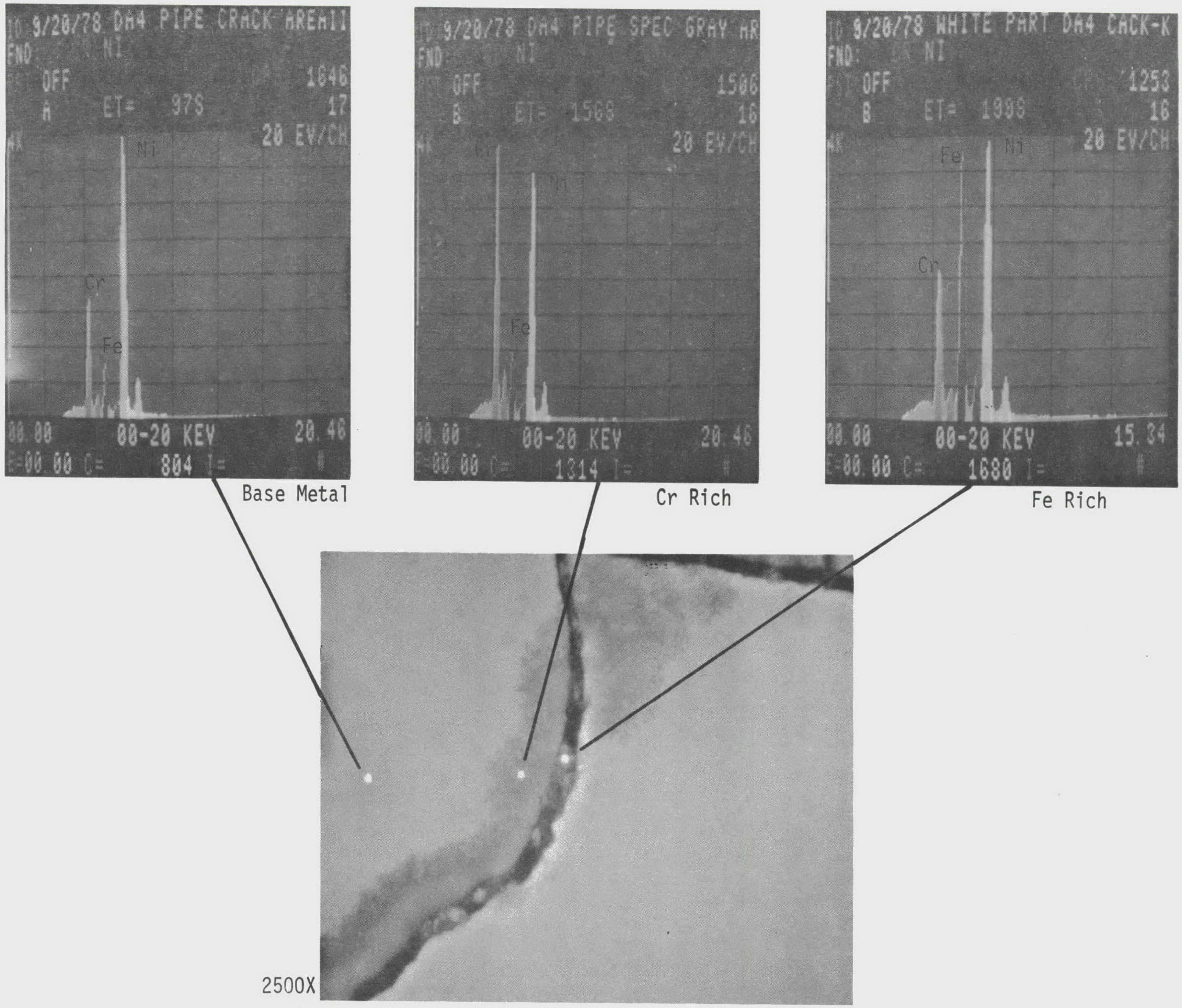

FIGURE 17. SEM MICROGRAPH AND CORRESPONDING EDAX ANALYSES FROM SAMPLE 4

Area shown is located within the rectangular region highlighted in Figure 6

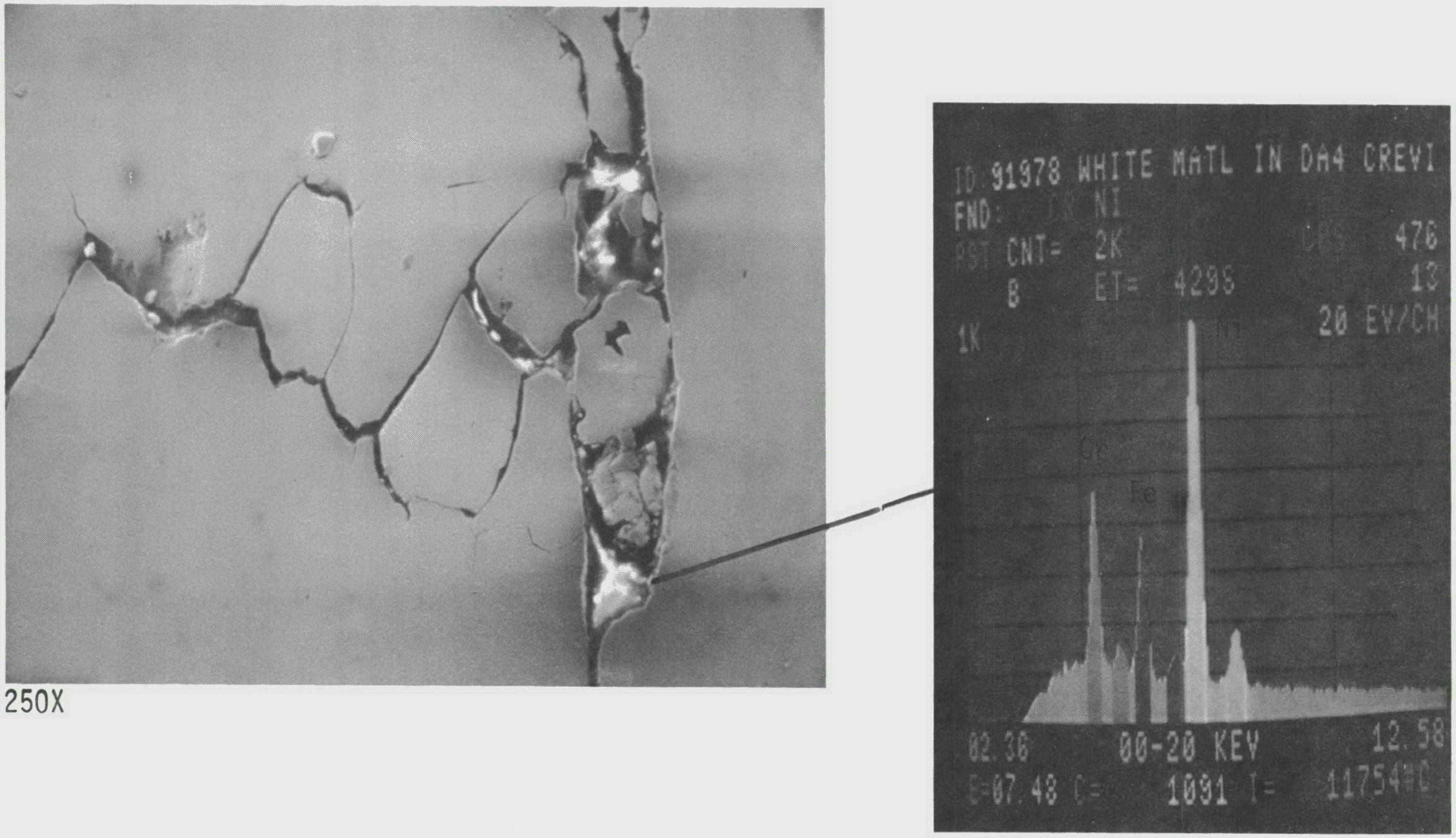

250X

FIGURE 18. SEM MICROGRAPH AND CORRESPONDING EDAX ANALYSIS OF IRON RICH MATERIAL IN CREVICE OF SAMPLE 4

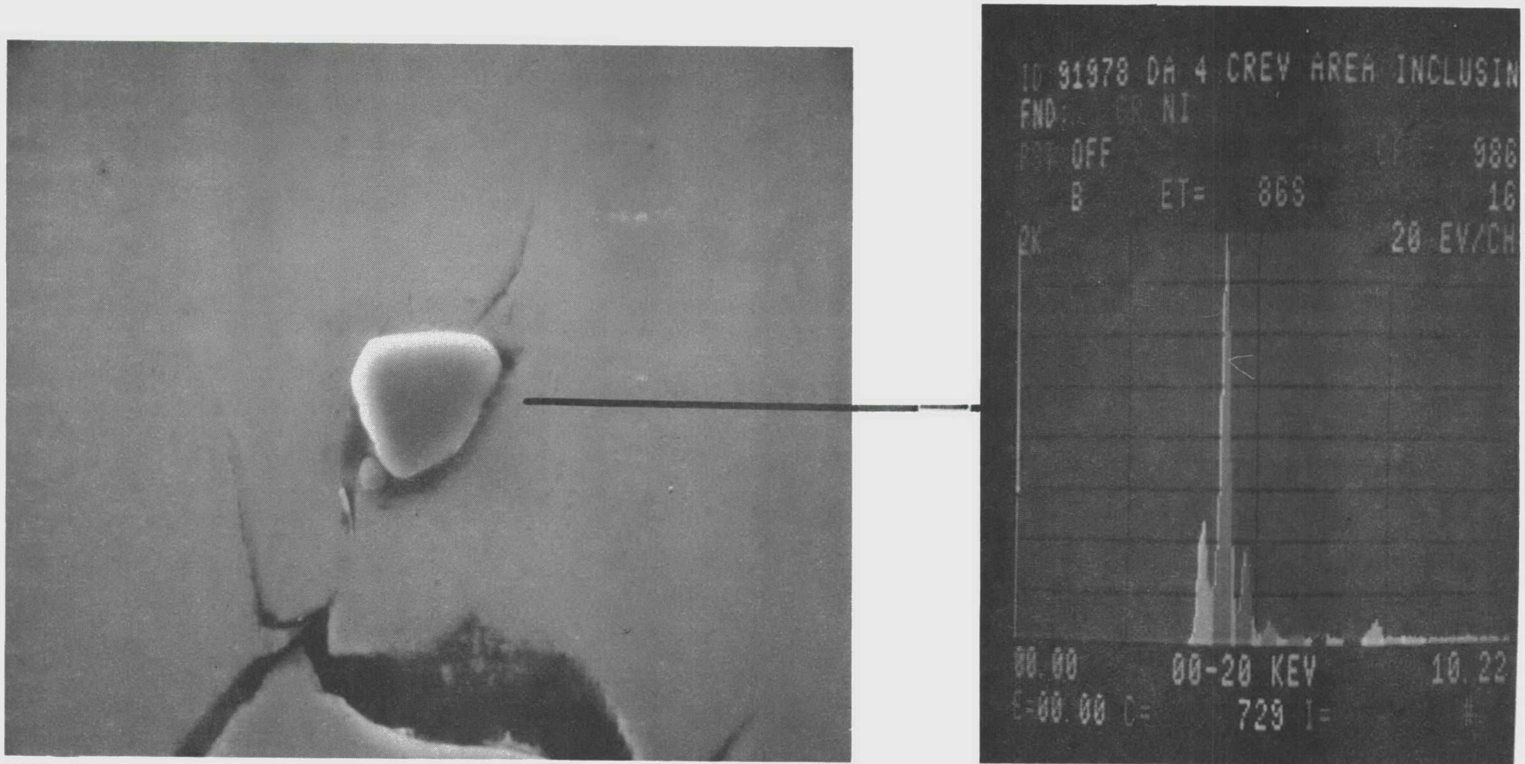

1600X

FIGURE 19. SEM MICROGRAPH AND CORRESPONDING EDAX ANALYSIS OF TITANIUM INCLUSION FROM SAMPLE 4

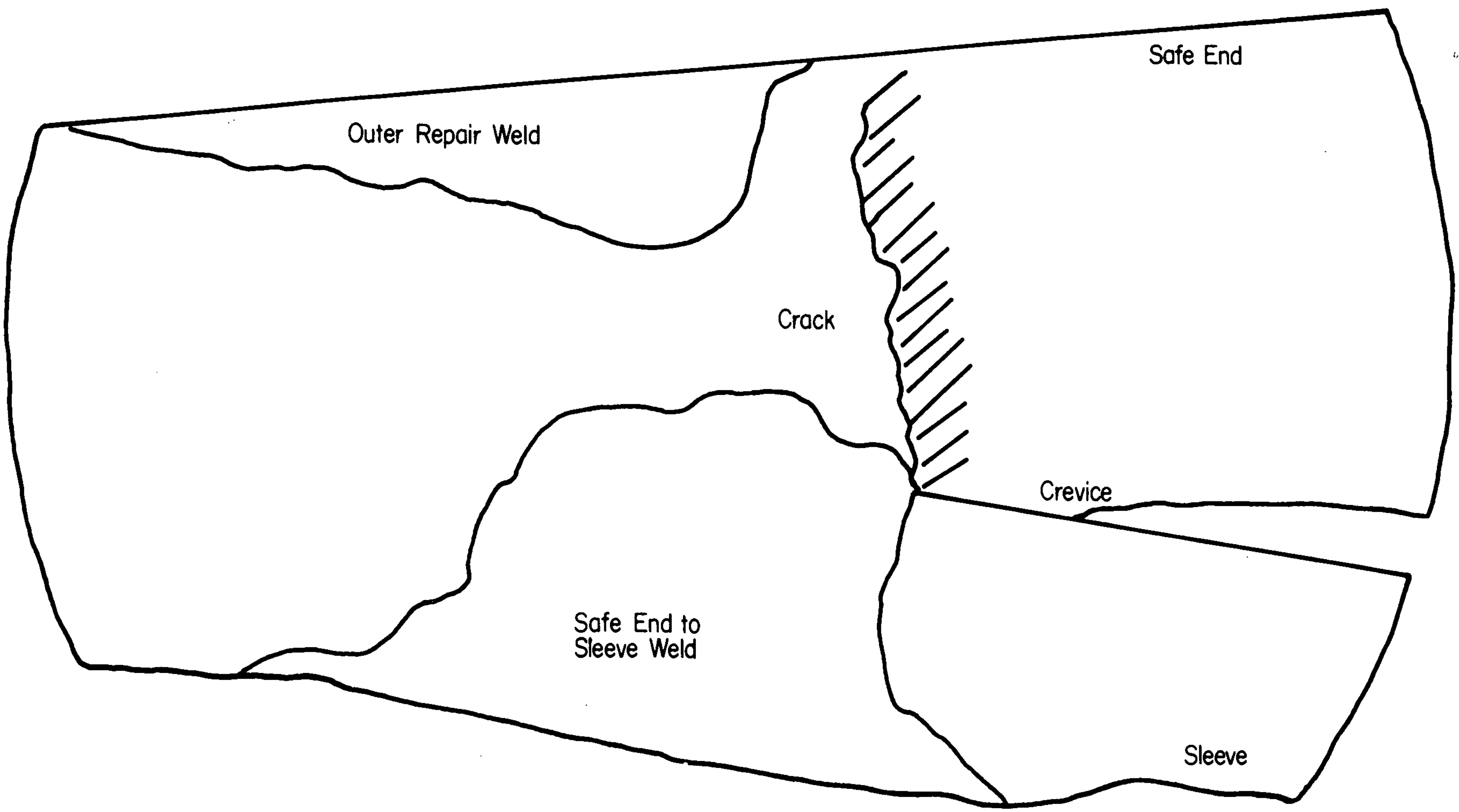

FIGURE 20. SCHEMATIC DIAGRAM OF SAFE END SAMPLE 5 INDICATING FRACTURE SURFACE EXAMINED BY SEM

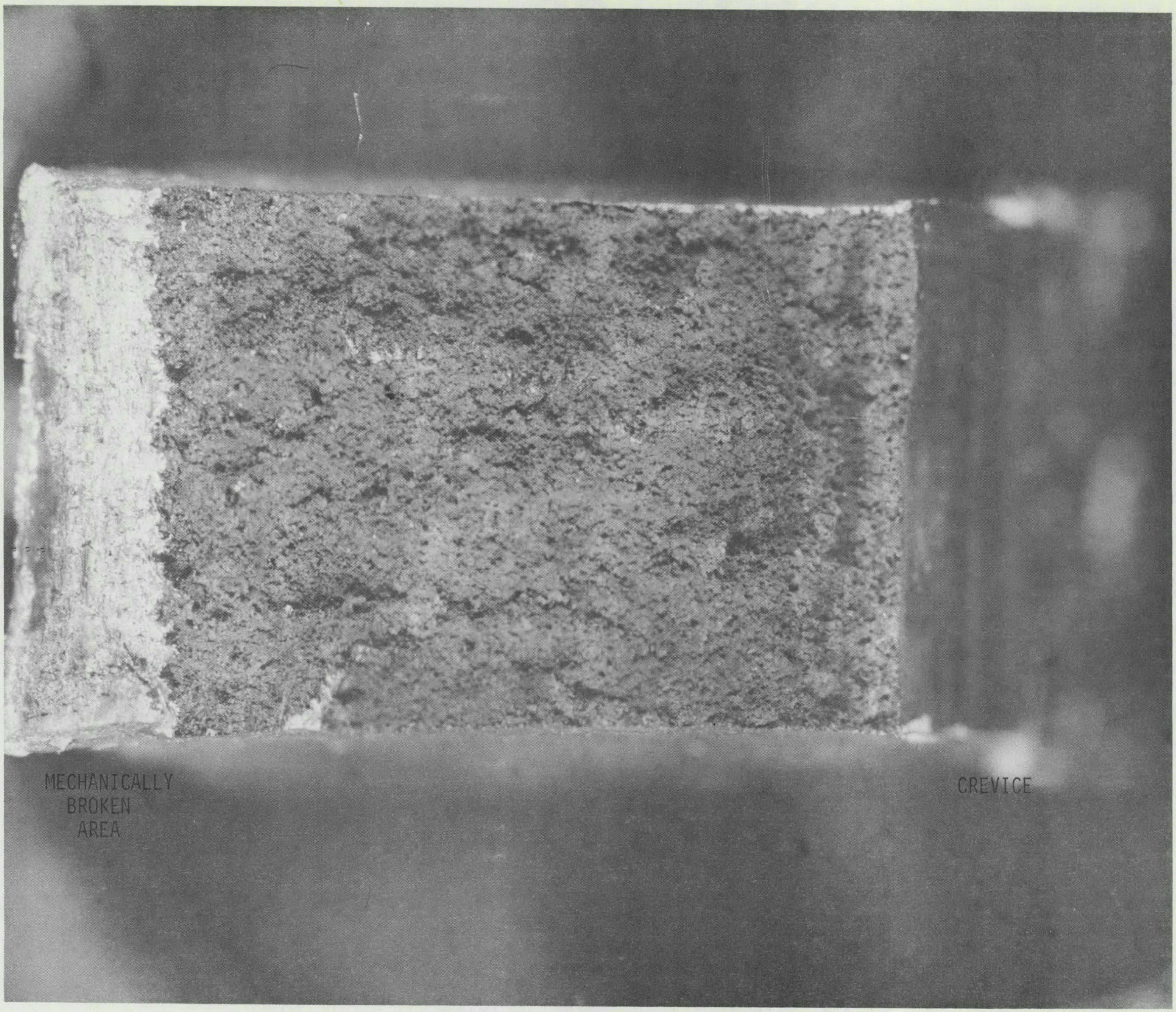

FIGURE 21. PHOTOMACROGRAPH OF FRACTURE SURFACE FROM SAMPLE 5

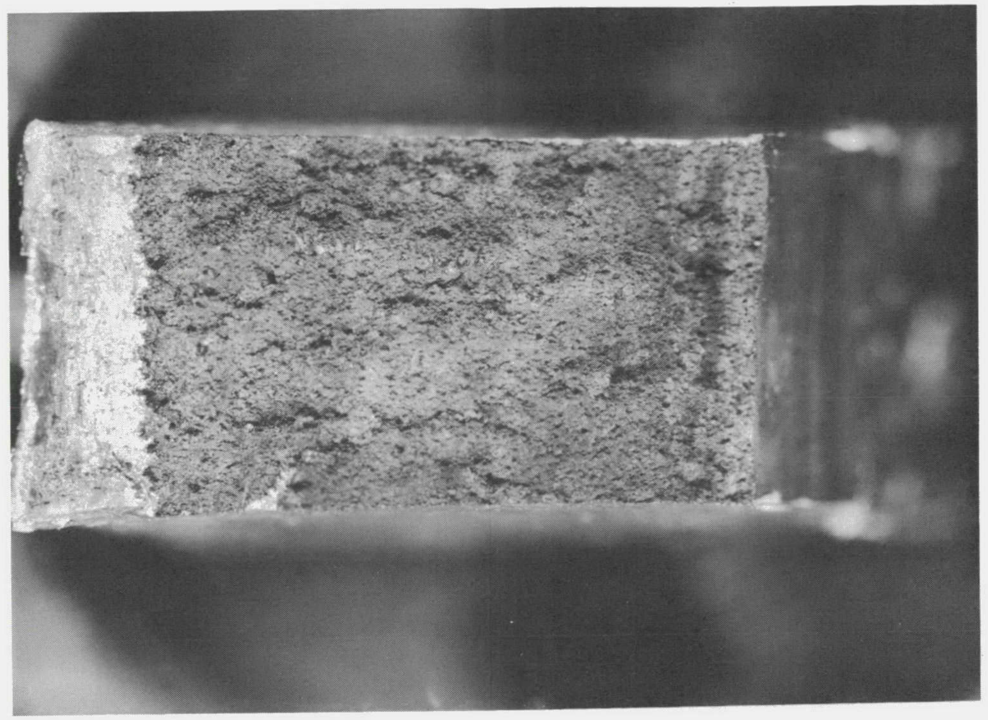

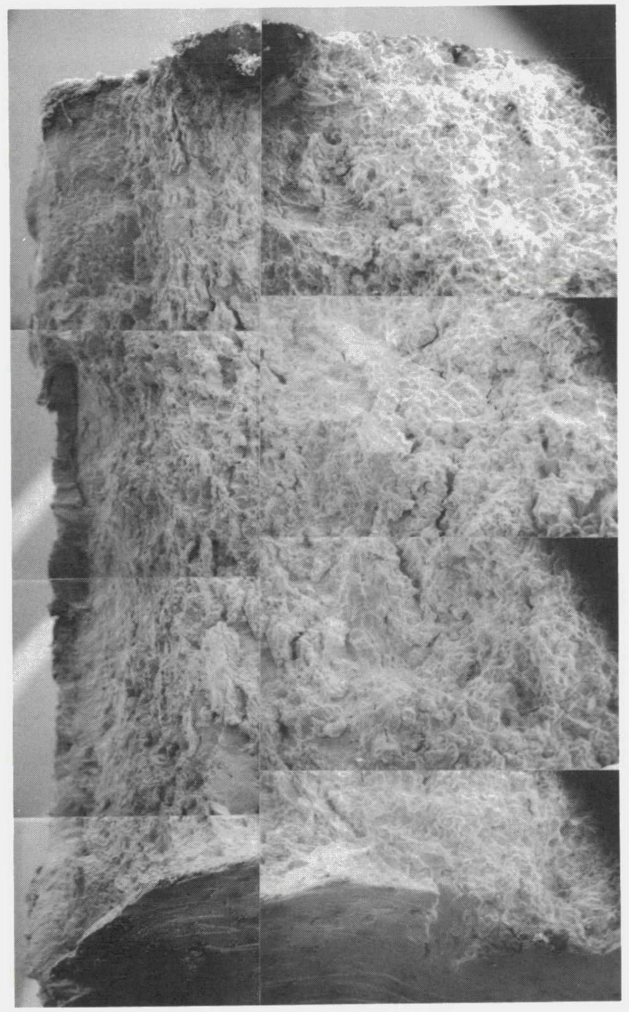

(a) Crack Tip

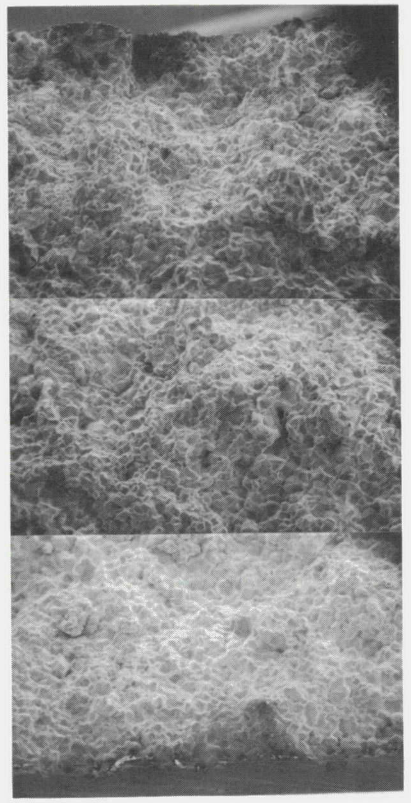

(b) Mid Fracture

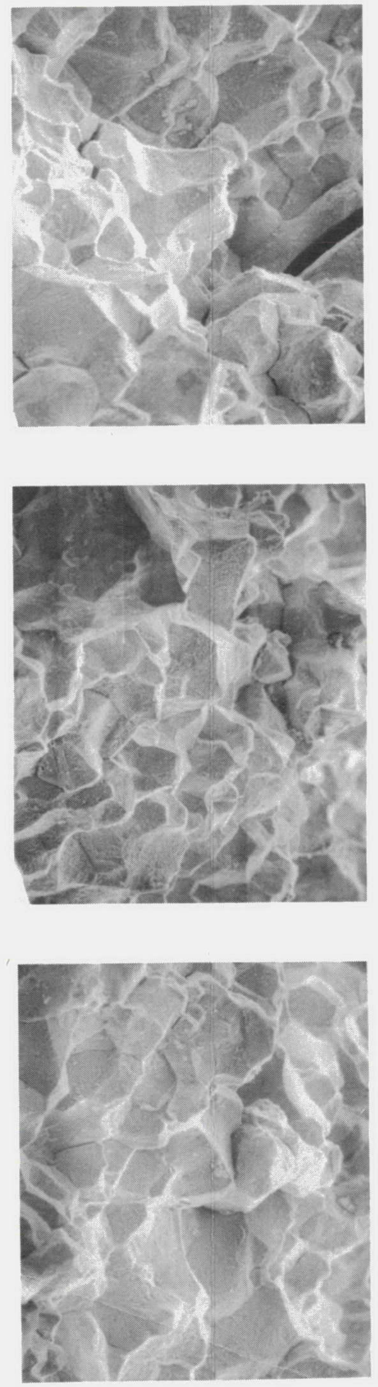

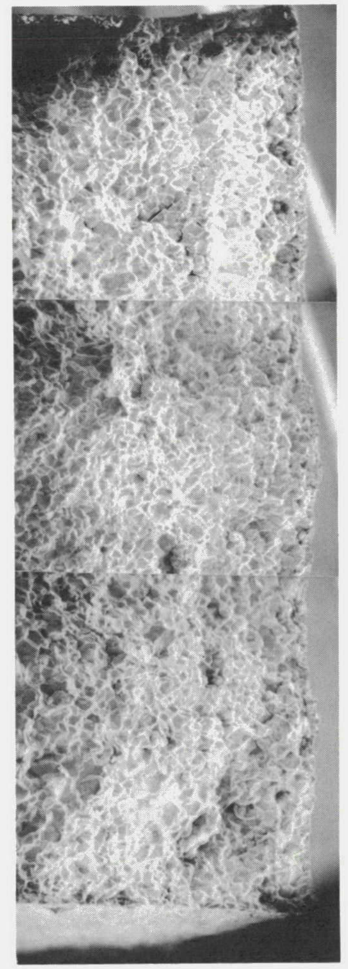

(c) Near Crevice

FIGURE 22. SEM MICROGRAPH MONTAGES OF SAMPLE 5 FRACTURE SURFACE (a) Crack Tip, (b) Mid Fracture, (c) Near Crevice

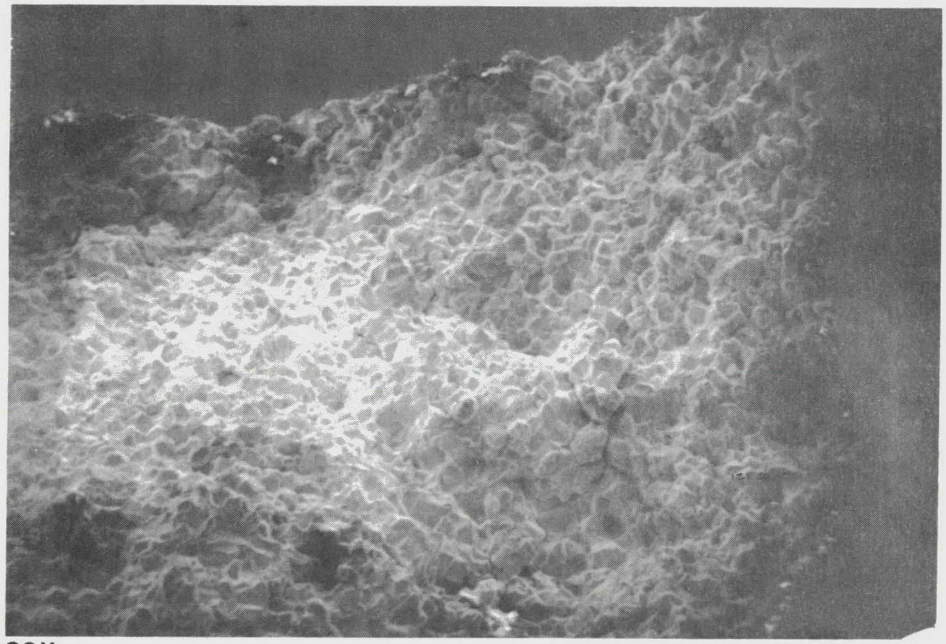

20X

(a) Typical area on fracture surface near crevice

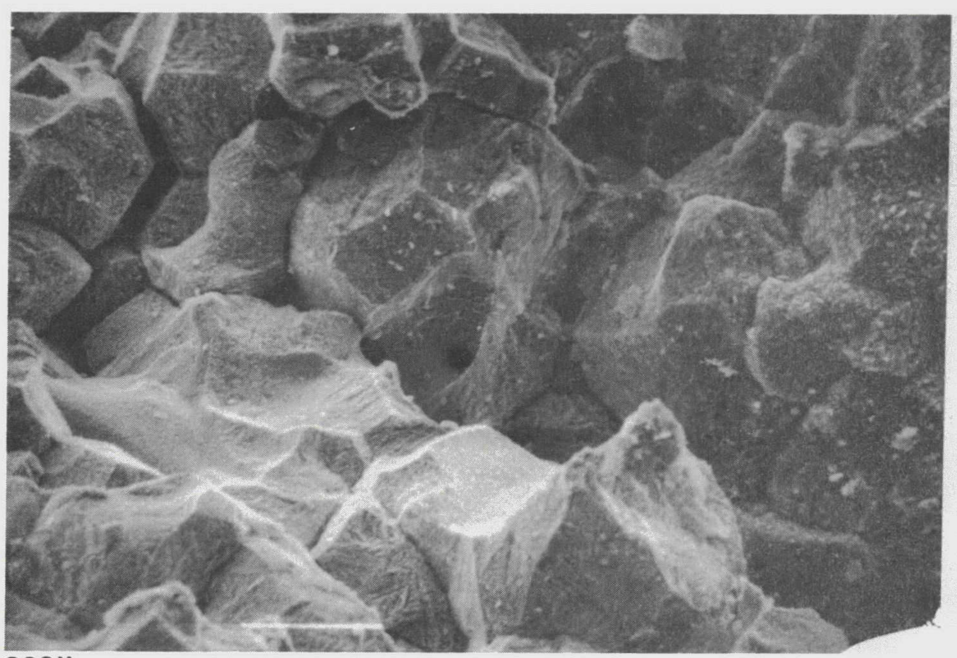

200X

(b) Actual area examined by EDAX analysis

FIGURE 23. SEM FRACTOGRAPHS OF SAMPLE 5 NEAR CREVICE

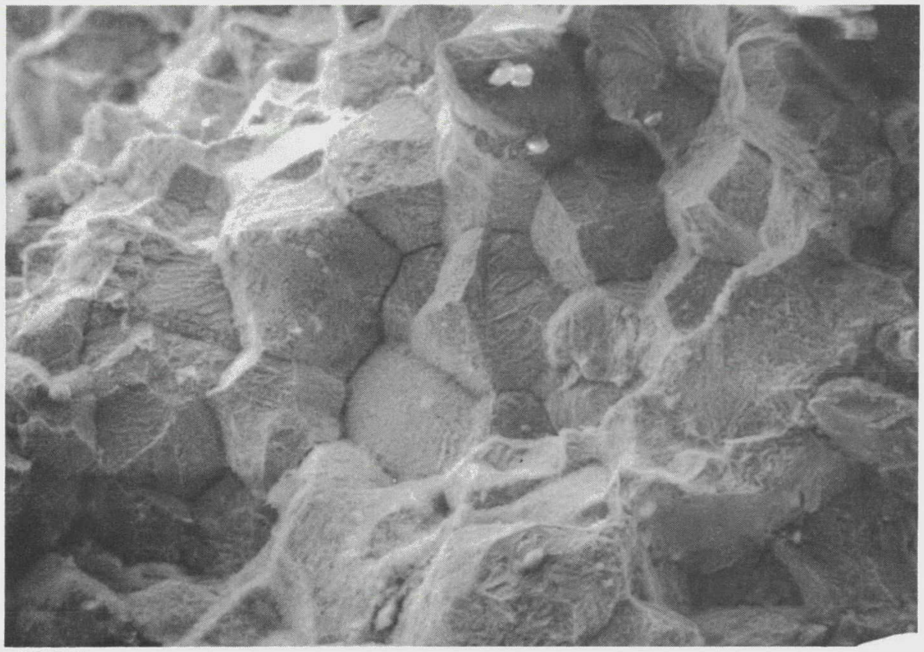

200X

(a) Actual area examined by EDAX analysis

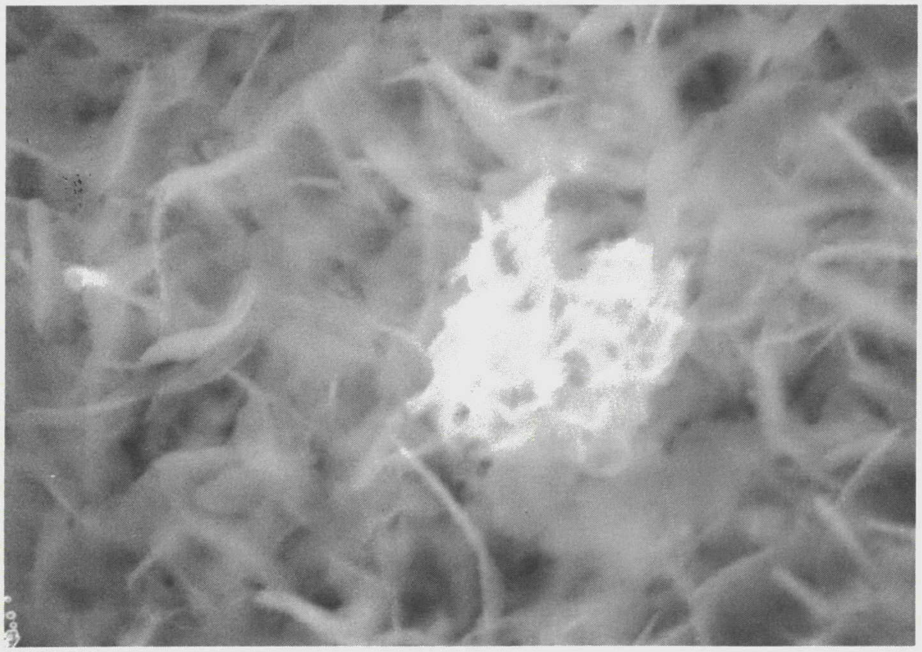

4500X

(b) Needle network of corrosion products on grain facet. Spot EDAX analysis indicated high sulfur content.

FIGURE 24. SEM FRACTOGRAPHS OF SAMPLE 5 AT MID FRACTURE

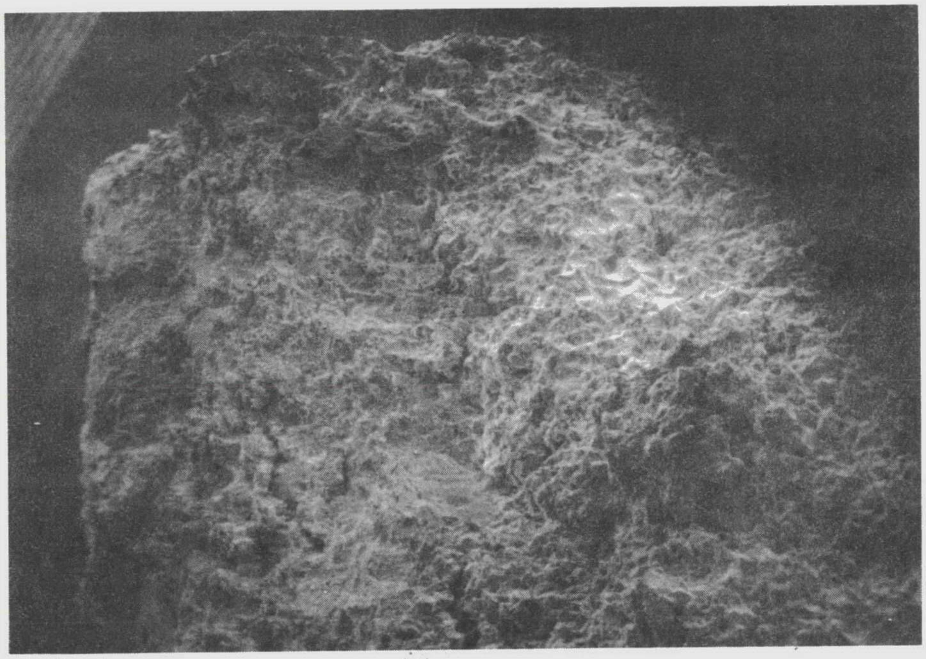

20X

(a) Typical area on fracture surface at crack tip.

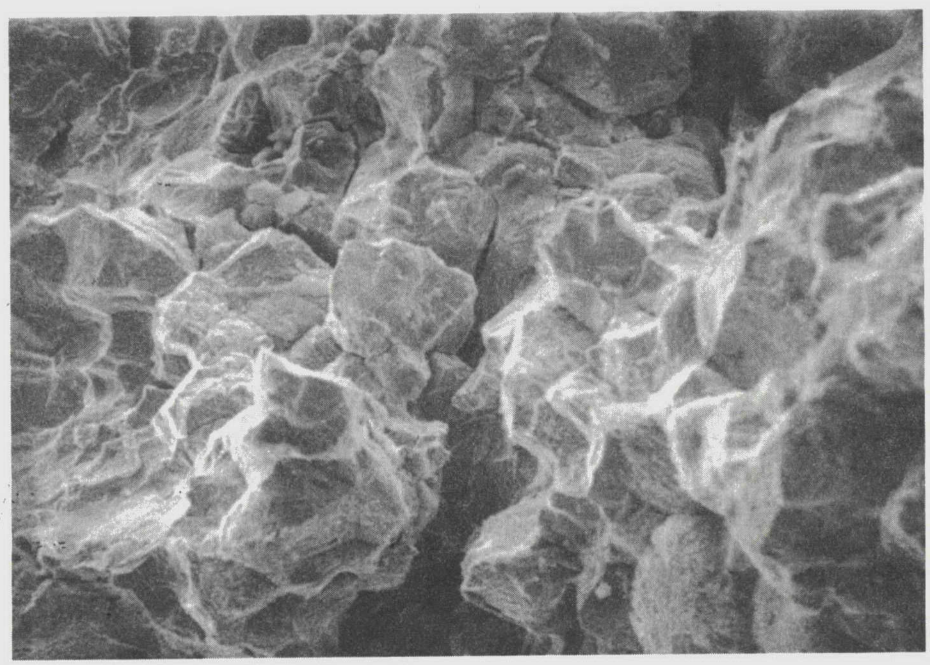

200X

(b) Actual area examined by EDAX analysis.

FIGURE 25. SEM FRACTOGRAPHS OF SAMPLE 5 AT CRACK TIP

Results from EDAX analysis of Figures 23, 24, and 25 and other areas not shown indicate no significant variations from base metal composition. However, small amounts of sulfur were detected in almost all of the fracture and crevice EDAX analyses. Figure 26 presents SEM micrographs taken on the fracture surface near the crack tip. The crystalline material, magnified to 2000X in Figure 26b, was subjected to spot EDAX analysis. Results indicate high sulfur contents (~8 times greater than the highest sulfur content detected in area EDAX scans on the fracture surface). Similar crystalline structures were observed and analyzed on the crevice surface, and they too indicated relatively high sulfur content.

In order to characterize the sulfur distribution along a fracture surface and determine the source of the sulfur contaminants Sample 1 was mechanically fractured in the same manner as Sample 5 and examined by SEM. EDAX analyses were performed along the fracture surface at designated intervals to quantify local sulfur concentrations. A total of 11 EDAX scans were performed along a radial axis from the crevice to the tip of the crack. In addition, two EDAX analyses were performed on the mechanically broken ductile material. Each EDAX scan examined in surface area of approximately 1.6×10^{-2} cm^2. The results of the EDAX analyses are presented as Figure 27. The relative sulfur concentration data presented in Figure 27 are plotted versus wall thickness. Based on this data an increase in relative sulfur concentration was observed with increasing crack penetration (with the exception noted directly at the crack tip). The relative sulfur concentrations measured in the ductile material beyond the crack tip indicate a significant concentration deviation from the fracture surface*. Based on the difference in relative sulfur concentrations on the fracture surface and the ductile material and the appearance of the sulfur rich particles and the high concentration of sulfur in them, it is believed that the source of sulfur in the cracks was external to the base metal material.

---

*It should be noted that sulfur concentration shown for the base material are intended only for comparison with those in the fracture surface. The values should not be taken as representative of actual sulfur concentration in the base metal. (See Table 3 for sulfur content in base metal.)

50X

(a) Cluster of crystalline material near crack tip.

2000X

(b) Crystalline material subject to EDAX spot analysis. Results indicate high sulfur content (>20%).

FIGURE 26. SEM FRACTOGRAPHS OF SAMPLE 5 NEAR CRACK TIP

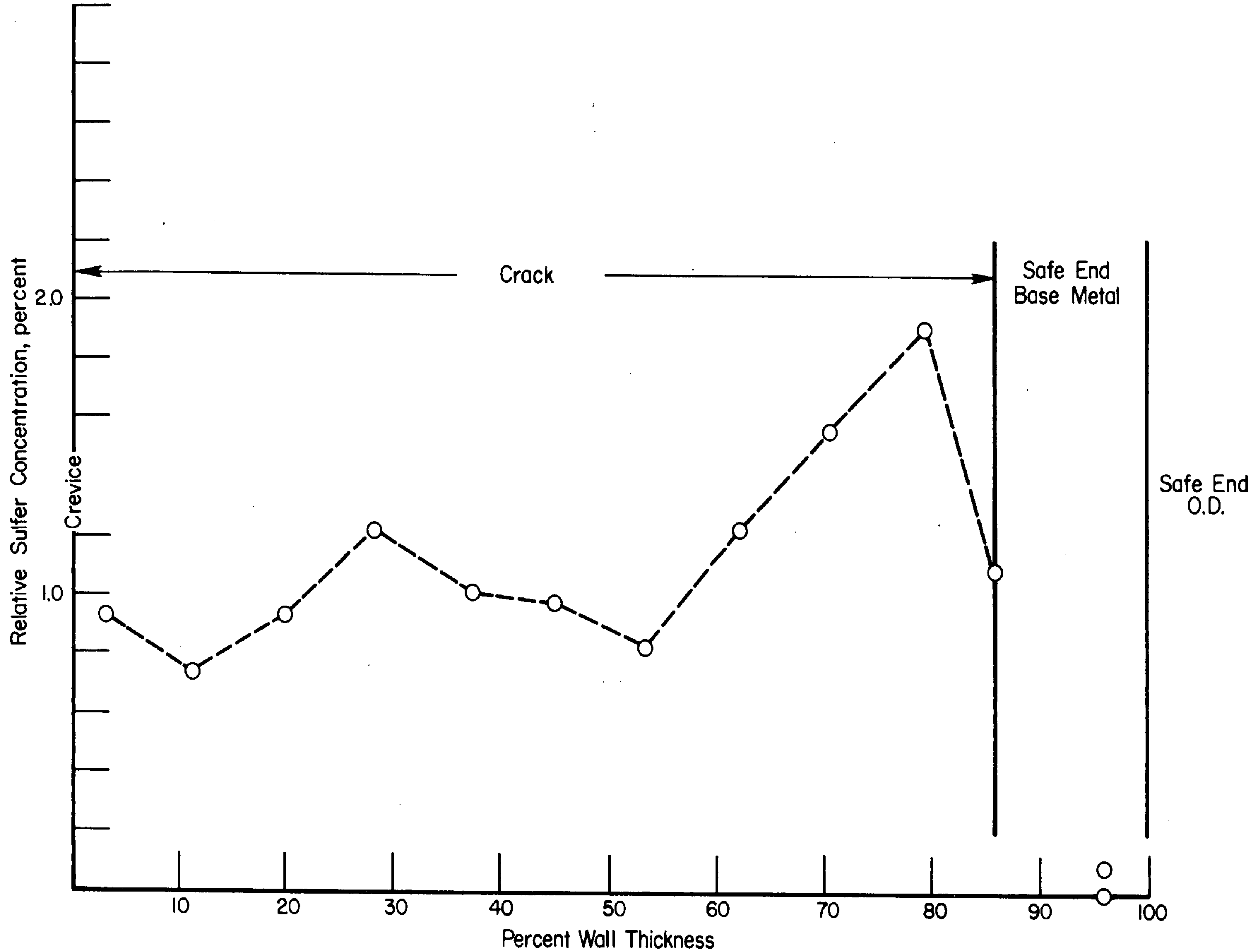

FIGURE 27. DUANE ARNOLD SAFE END SULFUR PROFILE ON FRACTURE SAMPLE No. 1

2.8 Electron Microprobe (EMP) Analysis of Duane Arnold Sample No. 2

Sample No. 2 was examined in detail with the electron microprobe. Examination consisted of 2Θ scans, X-ray mapping and area or point counting. Areas analyzed included base metal, grey phase, and weld metal. In preparation for semiquantitative analysis the sample was mounted in a stainless steel ring with epoxy, ground with SiC papers and polished with Al_2O_3 powder.

Two theta scans were obtained for each area by simultaneously scanning with LiF, PET, and KAP crystals to analyze elements from $_{11}$Na through $_{94}$Pu. In addition to the major elements Ni, Cr, and Fe, traces of Ti and Si were noted in the base metal and grey phase-crack areas. The weld metal indicated a minor amount of Mn. Results are tabulated in Table 4.

Fixed time (30 sec) area counts were then performed on the same three areas for Ni, Cr, and Fe to obtain semiquantitative analyses. The results are shown in Table 5. By comparison with pure standards, results on a first-approximation basis (e.g., no corrections for atomic number, absorption or fluorescence) were obtained. Base metal results are shown to agree reasonably well with the nominal and analytical chemistry results. Of main importance is the Cr increase in the grey phase by ~50% (relative). This analysis supports the qualitative results obtained in the scanning electron microscope (SEM).

X-ray mapping, as shown in Figure 28, compares the Ni, Cr, and Fe distribution in a grey phase-crack location. For orientation purposes the X-ray images must be compared with the electron backscatter (EBS) image, which in turn can be compared with the adjacent photomicrographs. The Ni X-ray map shows a decrease in Ni content in the Cr rich phase. The Cr image appears to indicate a slight intensity increase. Iron appears to follow the general area topography with relatively uniform distribution.

3.0 SUMMARY OF OBSERVATIONS AND CONCLUSIONS

An examination of the data presented in Section 2.0 of this report leads to the following observations and/or conclusions.

- All samples taken from the safe end and examined either by optical metallographic or SEM techniques contained part-wall cracks. No cracks were observed to penetrate the repair weld on the outer surface.

TABLE 4. ELECTRON MICROPROBE RESULTS OF 2θ SCANS IN BASE METAL, GREY PHASE AND WELD METAL

	Base Metal Area 3	Grey Phase Area 1	Weld Metal Area 4
Elements Detected Listed in Order of Decreasing Intensity*			
Major (>300 cps)			
	Ni	Ni	Ni
	Cr	Cr	Cr
	Fe	Fe	Fe
Minor (50-300 cps)			
			Mn
Trace (<50 cps)			
	Mg	Mg	Mg
	Ti	Si	Ti
	Si	Ti	Sr
			Si
			Nb

*Elements $_{11}$Na through $_{92}$U.

TABLE 5. ELECTRON MICROPROBE ANALYTICAL RESULTS FOR Ni, Cr, Fe FROM AREA/POINT COUNTING IN BASE METAL, GREY PHASE (POINT), AND WELD METAL*

	Base Metal Area 3	Grey Phase Area 1	Weld Metal Area 4	Inconel 600 Nominal (ASM)	Chemical Analysis (Base)
Percent Ni	77	63	80	76.0	73.6
Percent Cr	15	24	17	15.5	15.6
Percent Fe	7	9	5	8.0	7.8
Total	99	96	102	99.5	97.0

*First approximation results do not include atomic number, absorption, or fluorescence corrections.

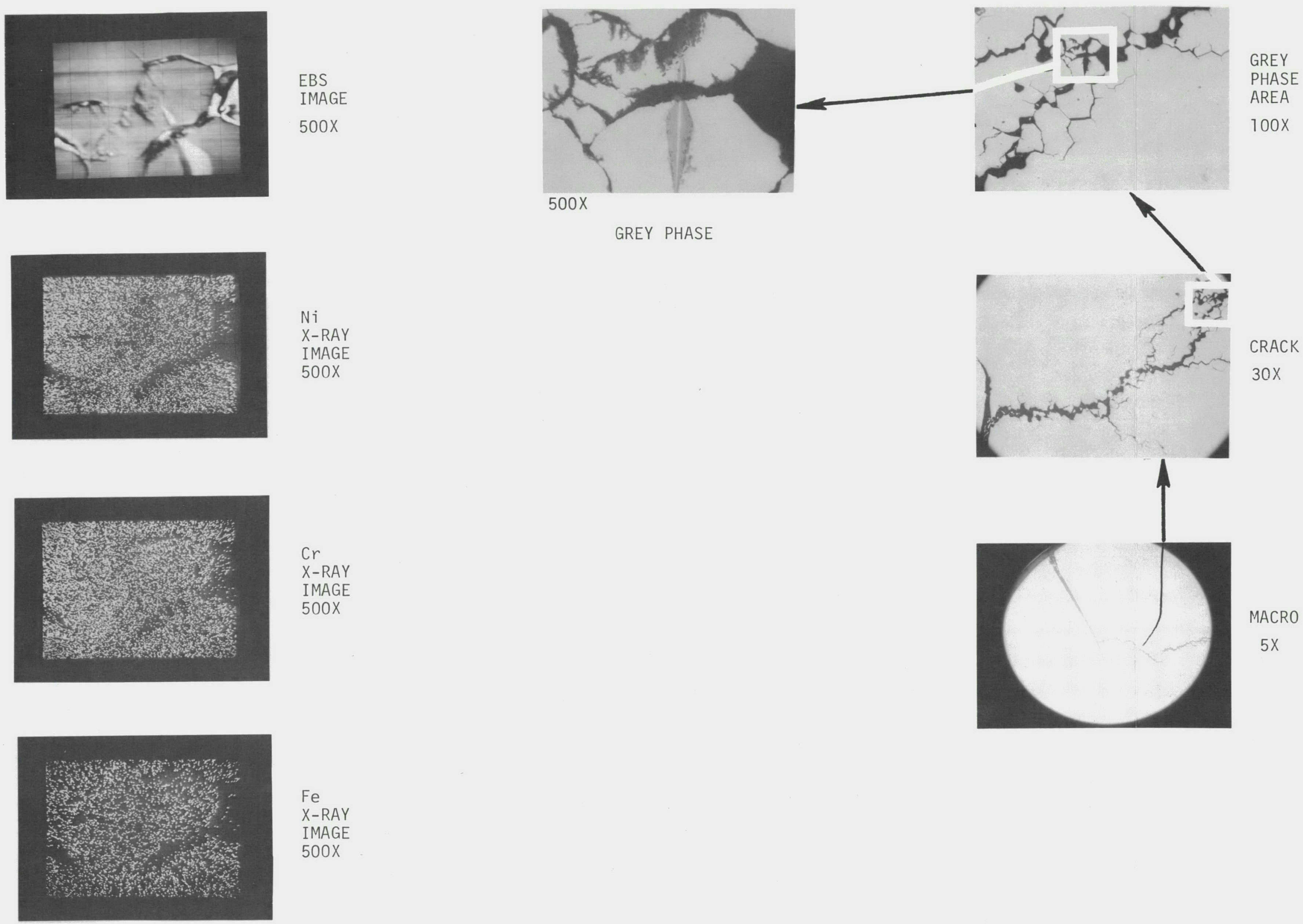

FIGURE 28. SAMPLE #2 - MICROPROBE RESULTS

- In all samples, the crack originated in the crevice between the sleeve and the safe end and radiated outward. No cracks were observed in the sleeve.
- The location of the cracks in all cases were in the re-solution treated region of the heat affected zone of the weld joining the safe end to the sleeve. See Figures 9 and 11.
- In the three samples examined metallographically, only one defect, namely the crack, was observed. No other crack precursors such as pitting were evident in the crevice region of any of the samples.
- All the cracks observed by metallography and fractography exhibited typical characteristics of intergranular stress corrosion cracks observed in nickel base alloys.[2-5]
- The depth of crack penetration in four of the five samples was about 80% of the safe end wall thickness. In the fifth sample which was taken from the opposite quadrant, the depth of crack was about 30%.
- From the location of the cracks, it is believed that the cause of crack initiation and subsequent propagation is not related to the repair weld on the outer surface of the safe end.
- The chemical composition of the safe end was within specification limits.
- Results of tensile tests on specimens from the safe end show no abnormalities.
- In all of the metallographic samples, small grey areas were observed around many tight branches of the cracks. These areas were found to contain relatively higher amounts of chromium. The source of the grey phase or its relationship to the cracking mechanism is not known.

- Small amounts of sulfur were detected in almost all of the fracture surface and crevice EDAX analyses. Relatively high sulfur content was detected in a crystalline appearing material near the crack tip on the fracture surface. No sulfur was detected on the metallographically prepared samples. From the appearance of the sulfur rich particles, the amount of sulfur in these particles and the concentration profile of sulfur on the fracture surface, it is believed that the sulfur was entrapped from the environment. However, it is not known if the presence of sulfur as a contaminant contributed to the cause of cracking.

REFERENCES

1. C. S. Tedmon, Jr., and D. A. Vermilyea, "Carbide Sensitization and Intergranular Corrosion of Nickel Base Alloys", Corrosion-Nace, 27, No. 9, pp 376-381, September (1971).

2. H. Coriou, L. Grall, P. Olivier, and H. Willermoz, "Influence of Carbon and Nickel Content on Stress Cracking of Austenitic Stainless Alloys in Pure or Chlorinated Water at 350 C", Proceedings of Conference Fundamental Aspects of Stress Corrosion Cracking, Columbus, 1967, Ohio State University, NACE (1969).

3. H. R. Copson and S. W. Dean, "Effect of Contaminant on Resistant to Stress Corrosion Cracking of Ni-Cr Alloy 600 in Pressurized Water, Corrosion, 22, pp 280-290 (1966).

4. H. A. Domian, R. H. Emanuelson, L. W. Sarver, G. J. Theus, and L. Katz, "Effect of Microstructure on Stress Corrosion Cracking of Alloy 600 in High Purity Water", Corrosion-Nace, 33, No. 1, pp 26-37, January (1977).

5. J. Blanchet, H. Corious, L. Grall, C. Mahieu, C. Otter, and G. Turluer, "Historical Review of the Principal Research Concerning the Phenomena of Cracking of Nickel Base Austenitic Alloys", Proceedings of Fifith European Congress of Corrosion, Paris, September (1973).